frontiers in Earth Science

ORIGINAL RESEARCH
published: 16 April 2021
doi: 10.3389/feart.2021.604520

A Juvenile Specimen of *Archaeorhynchus* Sheds New Light on the Ontogeny of Basal Euornithines

Christian Foth[1]*, *Shiying Wang*[2], *Frederik Spindler*[3], *Youhai Lin*[4] and *Rui Yang*[4]

[1]Department of Geosciences, University of Fribourg, Fribourg, Switzerland, [2]Institute of Vertebrate Paleontology and Paleoanthropology (CAS), Beijing, China, [3]Dinosaur Museum Altmühltal, Denkendorf, Germany, [4]Western Liaoning Museum of Paleontology, Liaoning Technical University, Fuxin, China

The ontogenetic development of extant birds is characterized by rapid growth, bone fusion and an early onset of flight ability. In contrast, little is known about how these ontogenetic traits evolved in the bird stem lineage, and the available data pertains primarily to Enantiornithes. Here, we describe an almost complete skeleton of a juvenile euornithine bird (LNTU-WLMP-18) from the Early Cretaceous Jiufotang Formation (Aptian), which was discovered near Lamadong Town (Jianchang County, Liaoning, China). Despite its completeness, bone preservation is rather poor. Thus, to increase the contrast between bone tissue and matrix, we used cyan-red-based autofluorescence photography. The specimen is more or less articulated and exposed in ventral aspect. The jaws are edentulous, the coracoid bears a procoracoid process, and the ischium lacks a proximodorsal process. The pedal unguals are short and barely curved, indicating a ground-dwelling lifestyle. Feathers, including long primaries, are present as carbonized traces. Several characters indicate that LNTU-WLMP-18 is a juvenile: the bone surface has a coarsely striated texture and no fusion is evident between the carpals and metacarpals, between the tibia and the astragalus and calcaneum, or among the metatarsals. Although juvenile characters have the potential to impede accurate identification of the specimen, morphological comparisons and cladistic analysis identify LNTU-WLMP-18 as most likely referable to the basal euornithine *Archaeorhynchus*, which would make the specimen the first juvenile bird from the Jehol Group that could be assigned to a specific taxon. Based on its size and the incomplete ossification of the bone surface, LNTU-WLMP-18 represents the smallest and therefore youngest known individual of this genus. A statistical comparison of limb proportions shows that the forelimbs of LNTU-WLMP-18 are significantly shorter than the hindlimbs, while the forelimbs are longer than the hindlimbs in subadult and adult individuals. This is different from the situation in some Enantiornithes, in which the forelimbs exceed the length of the hindlimbs even in hatchlings. Similar to Enantiornithes, *Archaeorhynchus* probably exhibit an early onset of flight ability, as indicated by the extensive wing plumage in LNTU-WLMP-18. Finally, the lack of gastroliths in the visceral cavity might indicate a dietary shift in *Archaeorhynchus* during ontogeny. As a small-bodied, ground-dwelling, seed-eating bird with a precocial ontogeny, *Archaeorhynchus* filled an ecological niche that later allowed early crown birds to survive the K-Pg mass extinction.

Keywords: Euornithes, ontogeny, Early Cretaceous, China, bird evolution

OPEN ACCESS

Edited by:
Corwin Sullivan,
University of Alberta, Canada

Reviewed by:
Sebastian Apesteguia,
Consejo Nacional de Investigaciones Científicas y Técnicas (CONICET), Argentina
Jingmai Kathleen O'Connor,
Field Museum of Natural History, United States

***Correspondence:**
Christian Foth
christian.foth@gmx.net

Specialty section:
This article was submitted to Paleontology, a section of the journal Frontiers in Earth Science

Received: *09 September 2020*
Accepted: *18 February 2021*
Published: *16 April 2021*

Citation:
Foth C, Wang S, Spindler F, Lin Y and Yang R (2021) A Juvenile Specimen of Archaeorhynchus *Sheds New Light on the Ontogeny of Basal Euornithines. Front. Earth Sci. 9:604520. doi: 10.3389/feart.2021.604520*

INTRODUCTION

Extant birds differ from other extant groups of amniotes (with the exception of Chiroptera) in having a unique anatomical bauplan that enables active erial locomotion (Brown 1963; Herzog 1968). In addition, they are characterized by a pattern of ontogenetic development that includes rapid growth, extensive bone fusion and onset of flight ability within the first weeks or months after hatching (Starck and Ricklefs, 1998a; Wang et al., 2019a; Plateau and Foth, 2020). The discovery of numerous ancestral birds from the Early Cretaceous of China (Benton et al., 2008; Zhou et al., 2010; Chiappe and Meng, 2016) and Spain (Sanz et al., 2002; Sanz et al., 2016) has provided new insights into the origin of modern birds and the evolution of feathers and flight (see Mayr, 2017; Wang and Zhou, 2017a, O'Connor, 2020 for summary), and to a lesser degree also into the evolution of their unique developmental mode. Macroevolutionary comparisons, for instance, indicate that the skull shape and small body size of extant birds probably result from paedomorphosis (i.e., the conservation of ancestral juvenile features in adults) nested deep in the evolution of Coelurosauria (Bhullar et al., 2012; Benson et al., 2014; Foth et al., 2016). In contrast, the intensity of bone fusion observed in this group and the rapidity of their growth reflect peramorphic heterochrony (i.e., the developmental exaggeration of ancestral adult traits), evolving within Ornithothoraces (Scheyer et al., 2010; Wang et al., 2017b; Plateau and Foth, 2020). Due to the rarity of juvenile avialan fossils, little is known about how these particular ontogenetic traits evolved in detail. Most available information comes from Enantiornithes (e.g., Elzanowski, 1981; Sanz et al., 1997; Chiappe et al., 2007; Xing et al., 2017; Kaye et al., 2019), an extinct subclade of ornithothoracines that represents the most diverse group of avialan stem birds during the Cretaceous (Wang and Zhou, 2017a). Enantiornithes show relatively slow skeletal growth (when compared with extant birds) in combination with an early onset of fledging, indicating a highly precocial developmental mode (Elzanowski, 1981; Sanz et al., 1997; Chiappe et al., 2007; Kurochkin et al., 2013). However, except for a limited number of specimens of *Gobipteryx* (Elzanowski, 1981), the juvenile enantiornithines that have been reported to date cannot be referred to any particular species. Thus, the documented ontogenetic changes represent only very general patterns.

Here, we describe the fossil remains of a juvenile avialan from the Early Cretaceous Jiufotang Formation (Aptian), which can be classified as a basal member of Euornithes (the ornithothoracine subclade that includes extant birds), and most likely a juvenile representative of the genus *Archaeorhynchus* (Zhou and Zhang, 2006). This new find allows for deep comparisons of juvenile morphology among enantiornithines, euornithines and more basal members of Avialae, giving new insights into the ontogenetic development of Mesozoic birds.

Geological Settings

The fossil described in this paper was collected by Prof. Yang Rui in the town of Lamadong, 21 km southwest of Jianchang, Jianchang County, Liaoning, China. The locality exposes the lower part of the Jiufotang Formation, which is Aptian (Early Cretaceous) in age (see Zhang et al., 2007; Cao and He, 2019) (**Figure 1**).

MATERIAL AND METHODS

Material

The specimen represents a single slab containing the remains of an immature bird fossil. It was found and mechanically prepared by one of the authors (YR). The counter slab was unfortunately lost, and is therefore not available for study. The specimen is housed at the Western Liaoning Museum of Paleontology (WLMP) of the Liaoning Technical University in Fuxin (LNTU), and stored under the collection number LNTU-WLMP-Yang Rui-18 (**Figure 2**; **Table 1**).

Autofluorescence Imaging

For photo documentation, we used a cyan-red-based autofluorescence technique (**Figure 2B**; **Figures 3A,B**) which increased the contrast between fossilized hard and soft tissues and the matrix, emphasizing delicate structures, cracks and preparation artifacts that were at best poorly discernible under visible light (Haug et al., 2011; Haug and Haug, 2011; Foth et al., 2020). The investigation was performed with a *Canon EOS 600D* camera and a *Canon Macro Photo Lens MP-E* 65 mm, equipped with a red filter foil taken from cyan-red stereo spectacles. The complementary cyan filter foil was attached to three LED light sources. After the specimen was excited by cyan light, only the emitted red light passed readily through the complementary red camera filter, while light of other wavelengths was mostly blocked (Haug et al., 2011; Haug and Haug, 2011). To increase the signal, the autofluorescence images were modified by deleting the blue and/or green color channels in *Adobe Photoshop CC 19.0* (Adobe Inc.) to increase the contrast between fluorescent and non-fluorescent structures.

Phylogenetic Analysis

For taxonomic identification, we added LNTU-WLMP-18 to the phylogenetic dataset recently published by Zheng et al. (2018). Characters that pertain specifically to the adult condition were scored as inapplicable for LNTU-WLMP-18. The species sample in the dataset was modified, following a recent taxonomic revision of Confuciusornithidae that found *Jinzhouornis yixianensis* to be a junior synonym of *Confuciusornis sanctus* (Wang et al., 2019a). Furthermore, *Didactylus jii* was treated as a junior synonym of *Sapeornis chaoyangensis*, following Gao et al. (2012). The updated dataset consisted of 62 terminal taxa scored for 245 characters (see **Supplementary Files S1**, **S2**) and was analyzed using the software TNT 1.5 (Goloboff, Farris and Nixon, 2008; Goloboff and Catalano, 2016), using equal weights and implied weights ($K = 12$; Goloboff et al., 2018) through a heuristic search of 1,000 replicates of Wagner trees, followed by TBR (tree bisection and reconnection) branch swapping.

Statistics

Limb proportions of LNTU-WLMP-18 were compared with those of previously described *Archaeorhynchus* specimens (see

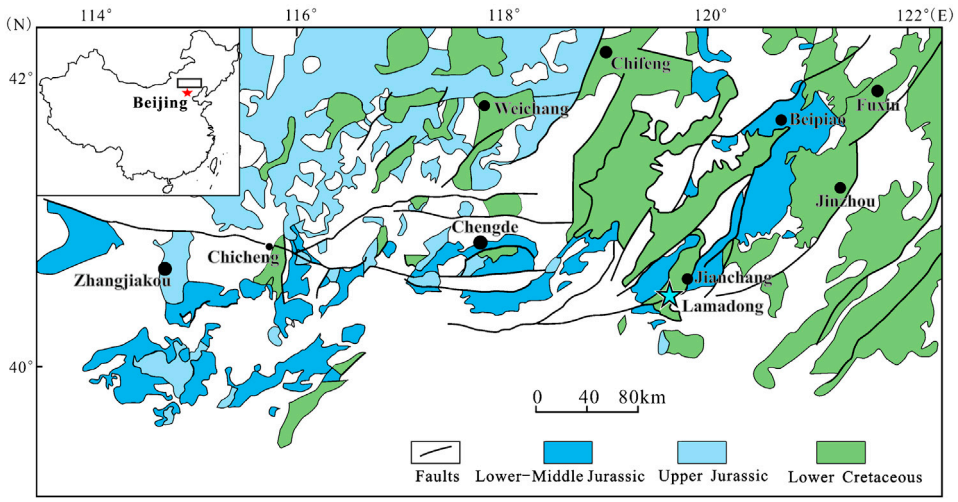

FIGURE 1 | Geological map of northeastern China (western Liaoning, northern Hebei and adjacent Inner Mongolia), showing the distribution of Late Mesozoic terrestrial strata and the geographic locality of LNTU-WLMP-18 near Lamadong Town (turquoize star). Modified after (Liu et al., 2012).

discussion for taxonomic classification) using the one sample *t*-test, which allows estimations of the probability that the two sets of values represent the same population (**Table 2**). Significant differences in limb proportions between LNTU-WLMP-18 and other *Archaeorhynchus* specimens can be interpreted as potential ontogenetic changes. Furthermore, we compared the ontogenetic changes in the lengths of the forelimb (defined by the length of the humerus and ulna) and hindlimb (defined by the length of the femur and tibia) in *Archaeorhynchus*, *Archaeopteryx* (data from Rauhut et al., 2018) and *Confuciusornis* (data from Chiappe et al., 2008), using ordinary least squares (*OLS*) regression analysis. Equality in the slopes of the single ontogenetic trajectories was investigated using a one-way ANCOVA, which tests for equality of means between univariate groups, using *F* statistics (Hammer and Harper, 2006). The tests were performed with the software *PAST 3.21* (Hammer et al., 2001).

Anatomical Nomenclature

Following the argument of Wilson (2006), we applied the anatomical and directional terms commonly used in anatomical descriptions of non-avialan dinosaurs, rather than rigorously using the anatomical terms recommended in the *Nomina Anatomica Avium* by Baumel and Witmer (1993). However, the latter are for anatomical structures that are typical for extant birds, but not present in non-avialan dinosaurs. One major conflict between the two different nomenclatures pertains to the digit identity of extant birds and non-avialan tetanurans. While the three-fingered hand of tetanurans evolved through the successive reduction of digits V and IV in early theropod evolution, leaving digits I to III (e.g., Rauhut, 2003), embryological studies on the limb development of birds indicate digit primordia are most approproately identitied as II to IV (e.g., Hinchliffe and Hecht, 1984; Burke and Feduccia, 1997). This contradiction between palaeontological and embryological data renewed the controversy regarding the dinosaur origin of birds (Burke and Feduccia, 1997; Feduccia et al., 2005). To avoid this conflict in digit numbering, Baumel and Witmer (1993) suggested calling the three fingers of extant birds the alular digit, major digit and minor digit. However, new developmental studies indicate a decoupling of the digit anlagen from the molecular mechanisms that pattern them. This frameshift results in an imposition of digit identities I, II and III on the digit anlagen II, III, and IV (e.g., Wagner and Gauthier, 1999; Vargas and Fallon, 2005; Tamura et al., 2011; Young et al., 2011), which is further supported by recent anatomical comparisons among theropod manus throughout evolution (e.g., Bever et al., 2011; Guinard, 2015). Therefore, we apply the general digit nomenclature of non-avialan theropods to highlight the dinosaur origin of extant birds. Furthermore, we prefer the terms "anterior" and "posterior" over "cranial" and "caudal" (as the latter terms could be potentially confused with anatomical regions of the skeleton), and refer to the different sides of long bones according to their orientation in the resting pose in a theropod dinosaur.

Anatomical Description

Due to general uncertainty regarding the taxonomic classification of juvenile specimens in the fossil record, especially within the clade Avialae, the morphology of LNTU-WLMP-18 is described at face value and compared with other bird species from the Jehol Group. The reasons, why this specimen most likely represents a juvenile of the euornithine bird *Archaeorhynchus* are documented in the Discussion, on the basis of detailed anatomical comparisons with various euornithine bird species and a phylogenetic analysis. After the taxonomic evaluation, morphological differences with other *Archaeorhynchus* specimens are discussed from the perspective of ontogeny.

General Preservation

Only the main slab of the specimen is available for study, while the counter slab is missing. The specimen is exposed in

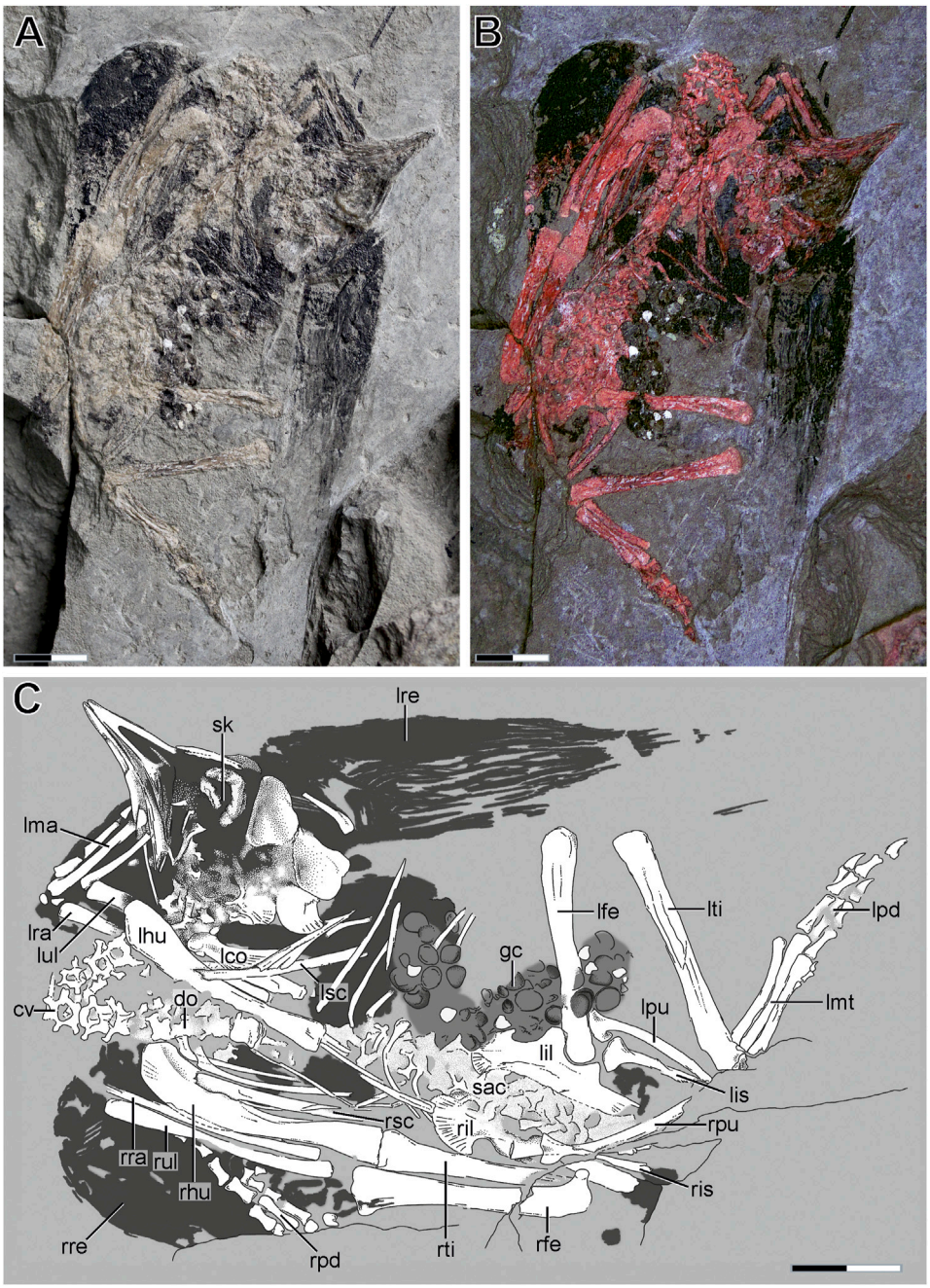

FIGURE 2 | Overview of the skeleton of LNTU-WLMP-18. **(A)** LNTU-WLMP-18 under normal light. **(B)** LNTU-WLMP-18 under cyan-red autofluorescence. **(C)** Explanatory drawing of LNTU-WLMP-18. Anatomical abbreviations: cv cervicals; do dorsals; gc gastric content; lco left coracoid; lfe left femur; lhu left humerus; lil left ilium; lis left ischium; lma left metacarpus; lmt left metatarsus; lpd left pedal digits; lpu left pubis; lra left radius; lre left remiges; lsc left scapula; lti left tibia; lul left ulna; rfe right femur; rhu right humerus; ril right ilium; ris right ischium; rpd right pedal digits; rpu right pubis; rra right radius; rre right remiges; rsc right scapula; rti right tibia; rul right ulna; sac sacrum; sk skull. Scale bar 10 mm.

ventral aspect, as indicated by the following spatial relationships: the right humerus covers the right scapula anteriorly; the left scapula is covered by the dorsal ribs; the right pubis covers the right ischium; and the preserved gut contents cover the dorsal ribs and the left femur (**Figure 2**).

In ventral view, the neck appears bent ventrally to the left side, while the head is exposed in right lateral aspect. The skeleton is more or less articulated, although some elements are displaced. The temporal region of the skull is disarticulated, but still in association with the rest of the cranium. The left humerus is rotated about its long axis and the right foot is incomplete and

TABLE 1 | Skeletal measurements of LNTU-WLMP-18 and other specimens of *Archaeorhynchus spathula*. *estimated values.

mm	LNTU-WLMP-18		IVPP V14287	IVPP V17075	IVPP V17091	IVPP V20312
	Left	Right		Zhou et al. (2013)		Wang et al. (2016)
Skull	>22.0	–	–	–	–	–
Scapula	>14.5	>15.0	46	46	43	–
Coracoid	8.0*	–	20	20	19	–
Humerus	20.5	22.0	54	53	49	59.1
Deltopectoral crest	NA	10.0*	–	–	–	–
Ulna	21.0	21.0	57	58	54	61.3
Radius	20.0	20.0*	56	55	52	60.3
Mc I	3.0	–	6	6	5	7.2
Mc II	11.0	–	25	25	23	–
Mc III	>7.5	–	24	23	21	–
MP I-1	5.0	–	10.5	10	9	–
PII-2	0.6*	–	–	12	10	–
Ilium	>16	20.5*	–	–	–	–
Pubis	>12.5	>16.0	37	28	30	–
Ischium	>8.0	10.0	20	17	14	–
Femur	21.0	21.5	37	36	34	–
Tibia	23.0	>18.0	43	42	39	44.9
Mt I	1.0	–	–	–	–	–
Mt II	10.0	–	–	–	–	–
Mt III	11.5	–	20	22	19	21.6
Mt IV	10.0	–	–	–	–	–
PP I-1	1.5	–	–	–	–	–
PP I-2 (U)	1.0	–	–	–	–	–
PP II-1	3.5*	–	–	6	5.5	–
PP II-2	2.5*	–	–	5	4	–
PP II-3 (U)	3.0*	–	–	5	4	–
PP III-1	4.0	–	–	6.5	6	–
PP III-2	2.5	–	–	5	5	–
PP III-3	2.5*	–	–	4	4	–
PP III-4 (U)	2.5*	–	–	5	4	–
PP IV-1	2.5*	–	–	5	4.5	–
PP IV-2	2.0*	–	–	3	3.5	–
PP IV-3	2.0*	–	–	2.5	3	–
PP IV-4	2.0*	–	–	2	3	–
PP IV-5 (U)	2.0	–	–	4	3.5	–

disarticulated from the tibia. However, phalangeal elements of the right foot can be found next to the right forelimb. Despite the general completeness of the specimen, some bones are hidden or missing, including various skull bones and the furcula, sternum (or anlagen for sternal ossification, see Zheng et al., 2012), sternal ribs, gastralia, right coracoid, right manus, and right metatarsus. Due to the loss of the counter slab, it is uncertain whether these bones were originally present or not. Unfortunately, the preservation of the remaining bones is rather poor. The limb bones are generally crushed and often split in half, so that the original cortical surface is not visible. However, these splits occur primarily in the midshaft regions of the bones, while the cortical surface of the proximal and distal ends remains intact (**Figure 3**). In addition, the specimen preserves the remains of the wing plumage and gut contents.

Ontogenetic Stage

Several characters indicate that LNTU-WLMP-18 is still a juvenile individual, which impedes taxonomic identification. As in extant birds and early juvenile non-avian theropods (Tumarkin-Deratzian et al., 2006; Chiappe and Göhlich, 2010; Dal Sasso and Manuco, 2011; Rauhut et al., 2012; Hone et al., 2016), the bone surface has a coarsely striated texture, which is associated with a high degree of vascularity resulting from increased rates of bone growth. Furthermore, the specimen lacks fusion between the carpals and metacarpals, among the tibia, astragalus, and calcaneum, and among the metatarsal bones, which are interpreted as juvenile characters in Ornithothoraces (e.g., Wang et al., 2017a; Wang and Zhou 2017b).

Skull

The skull of LNTU-WLMP-18 is heavily crushed (**Figures 4A,B**). During splitting of the rock, many skull bones were damaged or were lost with the counter slab. Consequently, the lacrimal, jugal, postorbital, squamosal, quadratojugal, quadrate, and palatal bones, as well as the basicranium, cannot be identified. Only the right **premaxilla** is exposed. LNTU-WLMP-18 possesses a short to moderately long edentulous beak (**Figures 3A**, **4A**,**B**), as in euornithines like *Archaeorhynchus* (Zhou and Zhang, 2006; Zhou et al., 2013), *Eogranivora* (Zheng et al., 2018), and *Schizooura* (Zhou et al., 2012). The premaxilla tapers anteriorly, with the nasal (frontal) process and maxillary

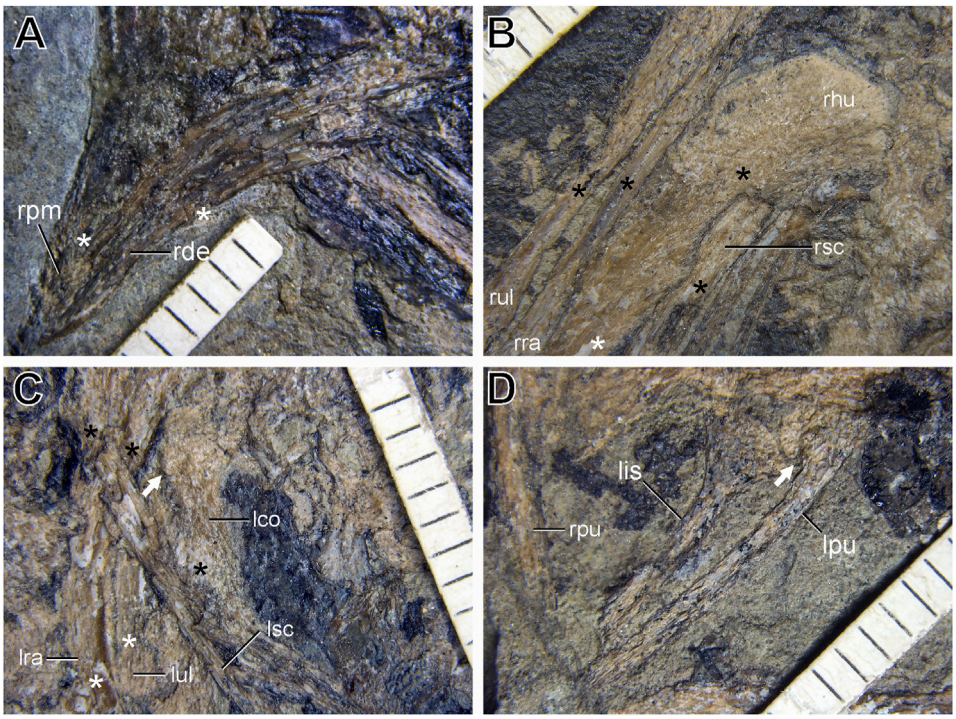

FIGURE 3 | Details of preservation of LNTU-WLMP-18 under normal light. White asterisks highlight regions, where long bones are split in half. Black asterisk highlight the original cortical structure of bones. **(A)** Close-up of the beak. **(B)** Close-up of the right forelimb. **(C)** Close-up of the left coracoid and forelimb. The white arrow highlights the procoracoid process of the coracoid. **(D)** Close-up of the pelvis. The white arrow highlights the ventral fossa between the ischial peduncle and pubic shaft. Anatomical abbreviations: lco left coracoid; lis left ischium; lpu left pubis; lra left radius; lsc left scapula; lul left ulna; rde right dentary; rhu right humerus; rpm right premaxilla; rpu right pubis; rra right radius; rsc right scapula; rul right ulna.

TABLE 2 | Comparison of skeletal proportions and statistical differences (*t*-test) between LNTU-WLMP-18 and other specimens *Archaeorhynchus spathula*. Comparisons with significant differences are shown in bold.

	LNTU-WLMP-18	IVPP V17091	IVPP V14287	IVPP V17075	IVPP V20312	*t*-value	*p*-value
Forelimb/Hindlimb	0.973	1.370	1.360	1.360	1.378	90.080	**<0.001**
Ulna/Humerus	0.988	1.102	1.056	1.094	1.020	4.230	**0.024**
Metacarpal-I/Humerus	0.141	0.102	0.111	0.113	0.122	−7.128	**0.006**
Metacarpal-I/Ulna	0.143	0.093	0.105	0.103	0.119	−6.870	**0.006**
Metacarpal-I/Metacarpal-II	0.273	0.217	0.240	0.240	0.277	−2.387	0.097
Metacarpal-II/Humerus	0.518	0.469	0.463	0.472	0.440	−7.780	**0.004**
Metacarpal-II/Ulna	0.524	0.426	0.439	0.431	0.431	−34.310	**<0.001**
Tibia/Femur	1.082	1.147	1.162	1.167	1.151	16.260	**<0.001**
Metatarsus-III/Femur	0.494	0.559	0.541	0.611	0.554	4.640	**0.019**
Metatarsus/Tibia	0.457	0.487	0.465	0.524	0.481	2.640	0.077

process diverging at an angle of approximately 20°. In (sub-)adult specimens of *Archaeorhynchus*, for instance, this angle measures approximately 30° (Zhou and Zhang, 2006; Zhou et al., 2013). The nasal (frontal) process is slender and elongated, forming the dorsal border of the external naris. Likewise, the length of the premaxillary body (measured as the distance between the anterior tip of the premaxilla and the anterior margin of the external naris) is considerable, measuring about 42% of the total length of the dorsal margin of the premaxilla (measured as the distance between the anterior tip and posterior end of the nasal process). The premaxillary body contributes the acute anterior apex of the external naris. The premaxilla is still in articulation with the anterior end of the **maxilla**, but due to compression, the suture between the two elements cannot be traced. Under autofluorescent light, a weak red light signal representing an upwardly directed process is detectable (**Figure 4B**), which could be either the ascending process of the maxilla or the anteroventral process of the right **nasal** that separates the external naris from the antorbital fenestra. Ventral to the nasal process of the premaxilla and dorsal to the possible ascending process of the

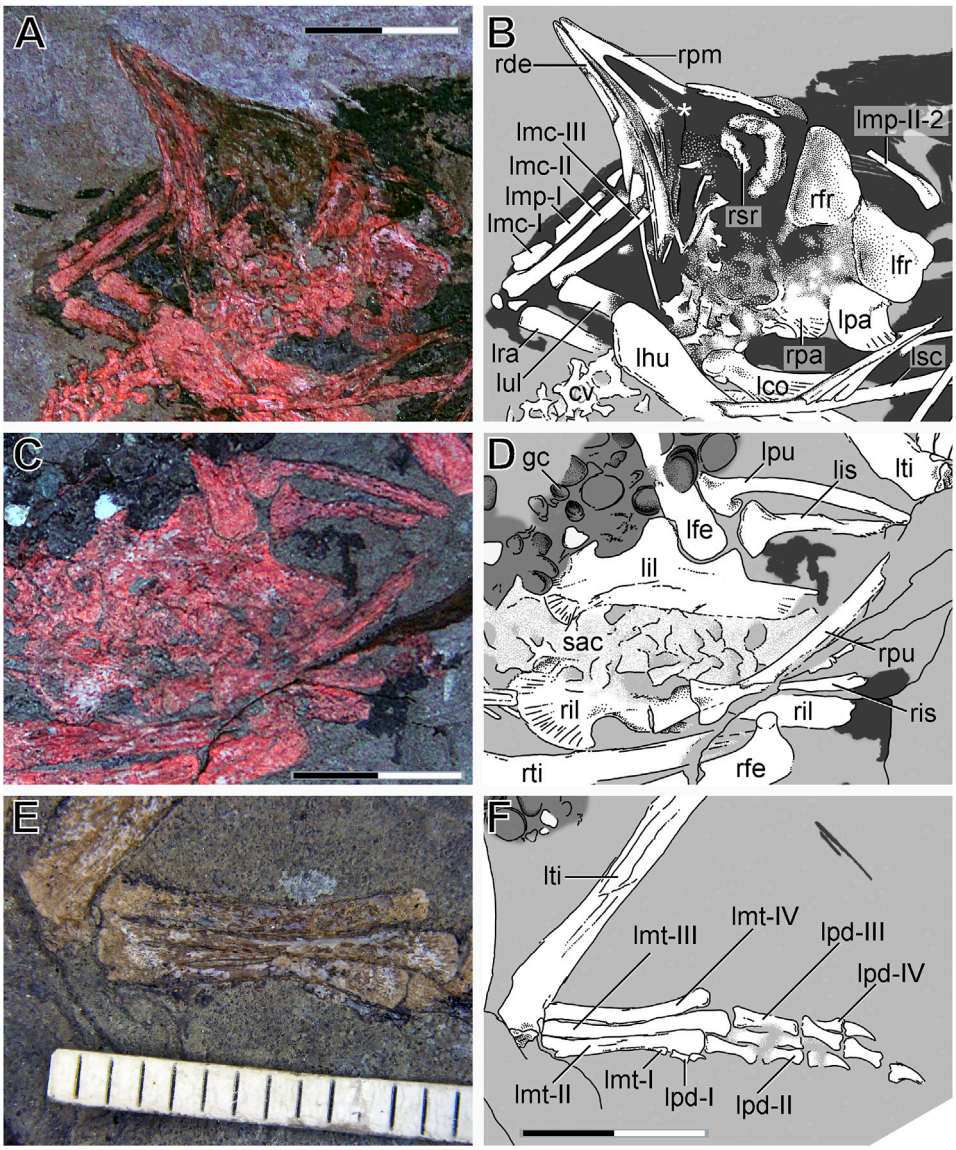

FIGURE 4 | Anatomical details of LNTU-WLMP-18. **(A)** Skull and left manus under cyan-red autofluorescence. **(B)** Explanatory drawing of the skull and left manus. The white asterisk marks the possible remains of the ascending process of the maxilla and the nasal body. **(C)** Pelvis and sacrum under cyan-red autofluorescence. **(D)** Explanatory drawing of the pelvis and sacrum. **(E)** Left metatarsus under normal light. **(F)** Explanatory drawing of the left foot. Anatomical abbreviations: cv cervicals; gc gastric content; lco left coracoid; lfe left femur; lfr left frontal; lhu left humerus; lil left ilium; lis left ischium; lmc left metacarpal; lmp left manual phalanx; lmt left metatarsus; lpa left parietal; lpd left pedal digits; lpu left pubis; lra left radius; lsc left scapula; lti left tibia; lul left ulna; rde right dentary; rfe right femur; rfr right frontal; ril right ilium; ris right ischium; rpa rigth parietal; rpm right premaxilla; rpu right pubis; rsr right scleral ring; rti right tibia; sac sacrum. Scale bar 10 mm.

maxilla, a further weak autofluorescence signal is present, which may correspond to remains of the nasal body. If these interpretations are correct, the two signals indicate the posterior and dorsal limits of the external naris.

The **frontals** are not fused to each other (**Figures 4A,B**), which represents the usual condition in non-ornithurine birds, including adult specimens of *Archaeorhynchus* (Wang et al., 2016; Plateau and Foth, 2020). The right frontal bone is more or less complete and exposed in laterodorsal view. As typical for avialans (e.g., Zhou et al., 2013; Wang et al., 2017a; Rauhut et al., 2018), it is elongated, forming the majority of the skull roof and the dorsal margin of the orbit. It narrows anteriorly and is still in articulation with the nasal process of the premaxilla, and the contact zone between both bones is marked by a distinct kink. The posterior portion of the right frontal, which is broken off and slightly displaced ventrally, is laterally expanded. The lateral margin of the posterior portion of the frontal bears an orbital rim, which is slightly offset from the dorsal roof of the frontals. Due to poor preservation, the anterior extent of the rim cannot be judged.

Posterior to the right frontal, remains of the left frontal are visible, with the element's concave ventral surface exposed.

Although the jugal and postorbital are missing, it is clear that the orbit was enlarged and rounded. In the center of the orbit, remains of a **sclerotic ring** are preserved (**Figures 4A,B**). While the dorsal half of the ring is more or less intact, the ventral part has suffered some damage. Ventral to the frontals, both **parietals** are preserved, and are fused neither to the frontals nor to each other. As with the frontals, the right element shows the external surface, while the right shows the internal one. Both elements are roughly square, but due to crushing and overlap with the anterior cervicals, no further details can be described. The absence of the postorbital bone could reflect imperfect preservation, but as this bone was lost independently in the enantiornithine and euornithine lineages (see e.g., Zhou and Zhang, 2006; O'Connor et al., 2010; Zhou et al., 2012; Zhou et al., 2014), its absence could also be genuine.

More than two-thirds of the **mandible** is preserved, with the posterior end missing (**Figures 4A,B**). In *Archaeorhynchus* the posterior end of the dentary is unforked (Zhou and Zhang, 2006; Zhou et al., 2013). Like in many other Jehol birds (Zhou and Zhang, 2006; O'Connor and Chiappe, 2011; O'Connor et al., 2011; Wang et al., 2017b), the ventral margin of the mandible is concave in shape. Only the anteriormost tip and the posterior end of the right **dentary** are preserved, while the mid-section is missing. Consequently, the left dentary is exposed in medial view, making it impossible to evaluate if the specimen possessed a longitudinal lateral groove with small foramina, as described for *Archaeorhynchus* and *Schizooura* (Zhou and Zhang, 2006; Zhou et al., 2012; Zhou et al., 2013). Nonetheless, the dentaries appear to be slender, spatulate, and edentulous as in *Archaeorhynchus* and *Schizooura* (Zhou and Zhang, 2006; Zhou et al., 2012; Zhou et al., 2013). Due to poor preservation, the remnants of the posterior part of the mandible are difficult to identify. Two small fragments lying posterior to the dentary probably represent the right **surangular** and **angular** in lateral view, while the posterior-most fragment might include remains of the right **prearticular** and the medial part of the left surangular (**Figures 4A,B**). However, nothing can be said about their morphology or that of the jaw joint.

Axial Skeleton

The vertebral column is poorly preserved. The more anterior cervicals are covered by the left humerus or intermixed with the crushed temporal skull bones so that nothing can be said about their anatomy or exact number (**Figures 4A,B**). The last seven posterior **cervical vertebrae** are preserved in association, but are no longer in full articulation. Due to rotation and displacement, one articular surface is exposed on each cervical, but it is not clear whether the anterior or posterior surface is exposed. The intense compression hampers morphological interpretation of the cervicals. Consequently, exact identification of particular processes is not possible. Due to the almost pentaradial arrangement of the processes, however, it is clear that the cervicals bear carotid processes, similar to *Archaeorhynchus*, *Schizooura*, and other Euornithes (Zhou et al., 2012; Zhou et al., 2013; Wang et al., 2016). The exposed neural canals are enlarged and rounded.

The **dorsals** and sacral series have both suffered much damage (**Figure 2**), and little can therefore be said about their morphology. The dorsal vertebrae seem not to be fused together, similar to other Early Cretaceous ornithothoracine birds (Clarke et al., 2006; Zhou and Zhang, 2006; Zhou et al., 2012; Zhou et al., 2014; Chiappe et al., 2020). Fine gaps between the vertebrae indicate that this was also true of the sacrals (**Figures 4C,D**). Due to damage and compaction, the exact number of sacrals cannot be determined. Neither **caudal vertebrae** nor a **pygostyle** are visible under normal light, although autofluorescent signals indicate that the fragmentary remains of some anterior caudals are present next to the right pubic shaft.

There is no indication of free **cervical ribs**. Many of the **dorsal ribs** are preserved in articulation with the dorsal section of the vertebral column. The ribs are long and straight and show no signs of **uncinate processes**, which are present in adult *Archaeorhynchus* (Zhou and Zhang, 2006) and many other Pygostylia (Chiappe et al., 1999; Zhang et al., 2001; Clarke et al., 2006; Wang et al., 2015). No **sternal ribs** or **gastralia** were identified.

Pectoral Girdle

Neither the **furcula** nor the **sternal elements** are preserved. This is also the case for the anterior and posterior ends of the left **scapula**. The anterior end of the right scapula is hidden by the overlying humerus, while the posterior end is not preserved. Thus, the only visible parts of the scapulae are the midshafts, which are very slender and straight. This is different from the condition in (sub-)adult specimens of *Archaeorhynchus* (Zhou and Zhang, 2006; Zhou et al., 2013) and other euornithine birds (Clarke et al., 2006; Chiappe et al., 2014; Wang et al., 2015), in which the shaft is slighty curved. The left **coracoid** is exposed in anterior view and lies in close association with the anterior end of the left scapula and the proximal end of the left humerus (**Figure 3C**). As preserved, the scapula and coracoid are unfused, which is the typical situation for Early Cretaceous ornithothoracine birds (Sereno et al., 2002; Clarke et al., 2006; Zhou and Zhang, 2006; Wang et al., 2016; Chiappe et al., 2020). The coracoid is a strut-like element. The omal end is relatively broad and forms a flattened, oval surface that faces laterally and might represent the articular facet for the scapula. Below the coracoid head a small, blunt tubercle is present on the medial side, which represents the procoracoid process (**Figure 3C**). This process is also present in *Archaeorhynchus* (Zhou et al., 2013), *Archaeornithura* (Wang et al., 2015), *Eogranivora* (Zheng et al., 2018) and *Yixianornis* (Clarke et al., 2006). The mid-section of the shaft is slightly constricted. Distally, the coracoid shaft expands drastically on the lateral side, while the medial expansion is minor. The lateral margin is almost straight and is longer than the medial one, similar to the condition in adult specimens of *Archaeorhynchus* (Zhou and Zhang, 2006). The distal expansion of the coracoid shaft indicates the presence of a broad contact zone for the sternum, but the actual sternal margin is damaged and cannot be evaluated (**Figures 4A,B**).

Forelimbs

Both forelimbs are preserved. The left **humerus** is turned 180° about its long axis, lying next to the dorsal column and exposing its posterior surface. The right humerus is preserved in natural position, exposed in anterior aspect (**Figure 2**). Proximally, the humeral head is craniocaudally convex and the internal tuberosity is not well developed. The small deltopectoral crest is only visible in the right element. As preserved, the crest measures more than one-third the length of the humerus, but its anterior margin is broken off, so that the actual shape cannot be evaluated. The middle part of the humeral shaft is almost straight, while the distal end is slightly expanded (**Figure 2**). The **ulna** is longer than the **radius**, but both bones are slightly shorter than the humerus, in contrast to (sub-) adult specimens of *Archaeorhynchus* (Zhou et al., 2012; Zhou et al., 2013) and many other euornithine birds (e.g., *Iteravis*, Zhou et al., 2014; *Bellulia*, Wang et al., 2016; *Eogranivora*, Zheng et al., 2018). The right ulna and radius are visible over their entire length, while the left elements are partly covered by the neck and by the left humerus, scapula and coracoid, so that only the proximal and distal ends are visible. As is evident from the right forelimb, the proximal end of the ulna is slightly expanded, but a distinct olecranon process is lacking as is typical for maniraptorans (Rauhut, 2003). The proximal half of the ulna is slightly bowed, and an interosseous cleft separates the ulna and radius over most of their length. The distal half of the ulnar shaft is almost straight, while the distal end is slightly expanded. In both forelimbs, the radius is displaced anteriorly with respect to the ulna. The former bone is straight and relatively thick, being more than half as wide as the ulna in the midshaft region (**Figures 2**, **3D**).

Only the proximal portion of the left **manus** is preserved, and the phalanges of the second (major) and third (minor) digit are covered by the skull (**Figures 4A,B**). Two ossified **carpal** elements can be identified, lying proximal to metacarpals II and III. They are similar in size and not fused to the metacarpals or to each other. This condition resembles the morphology of subadult specimens of *Archaeorhynchus* (Zhou et al., 2013), while adult specimens of ornithothoracine birds (including *Archaeorhynchus*) usually form a fused carpometacarpus (Wang et al., 2016; Wang et al., 2017b). Based on their positions, they most likely represent the semilunate carpal and the ulnare (Zhou et al., 2013). Traces in the rock might indicate that the radiale was also once present. A fourth carpal x (see Zhou et al., 2013) cannot be identified. **Metacarpals** I and III are slightly displaced distally, and are not in line with the proximal end of metacarpal II. The metacarpal elements are not fused to each other. The distal ends of metacarpal II and III are covered by the mandible, but the distal end of metacarpal II is visible due to a break in the jaw. Metacarpal I (the alular metacarpal) is short and rectangular, measuring less than one-third of the length of metacarpal II. No signs of additional processes, such as an extensor process or a pisiform process, can be identified. Metacarpal II is the most robust element in the metacarpus, and is almost straight. Its distal end is slightly expanded compared to the midshaft. Metacarpal III is approximately half as wide as metacarpal II. As its distal end is covered by the lower jaw, its actual length cannot be estimated. However, the bone is slightly bowed, forming a long intermetacarpal space. As preserved, the metacarpus of LNTU-WLMP-18 therefore resembles that of subadult individuals of *Archaeorhynchus* (Zhou et al., 2013).

Only in the first digit are the phalanges preserved in articulation (**Figures 4A,B**). The first **phalanx** of digit I is almost twice as long as metacarpal I. The remains of the first ungual indicate that this element was short and lacked a prominent flexor tubercle. It is very likely, also not certain that the first digit failed to reach the distal end of metacarpal II. As stated above, the phalanges of the second and third digits are covered by the skull. However, a single splint of bone preserved above the frontal (**Figures 4A,B**) might represent phalanx II-2. This bone measures approximately half the length of metacarpal II and shows a very distinct shape, with one end significantly expanded compared to the other. In ornithothoracine birds, the proximal third of phalanx II-2 exhibits a small posterior flange (e.g., *Archaeorhynchus*, Zhou et al., 2013; *Yanornis*, Wang et al., 2013b; *Sinornis*, Sereno et al., 2002), which could correspond to the expansion found in the element in question.

Pelvic Girdle

Both **ilia** are preserved, and exposed in medial view (**Figures 4C,D**). They are still in association with the sacrum, but not fused to the vertebrae. The right ilium is more or less complete, but its acetabular region is covered by the right pubis and ilium, and is separated from the postacetabulum by a deep crack in the matrix. In the left ilium the acetabular region is intact, but the anterior end of the preacetabulum is partly covered by gut contents (see below), while the posterior end of the postacetabulum is damaged. The preacetabulum seems to be as long as, or slightly longer than, the postacetabulum, but the exact ratio cannot be measured with certainty due to poor preservation. As in other euornithines, including subadult *Archaeorhynchus*, the preacetabulum is approximately twice as high as the postacetabulum (Zhou et al., 2013; Zhou et al., 2014). The preacetabulum possesses an rounded anterior margin, and shows a ventral expansion in the form of a prominent hook as seen in subadult specimens of *Archaeorhynchus* (Zhou et al., 2013), but also *Dingavis* (O'Connor et al., 2016), *Eogranivora* (Zheng et al., 2018), *Schizooura* (Zhou et al., 2012), and *Yixianornis* (Clarke et al., 2006). Furthermore, the preacetabular blade shows a radial pattern of strong striations. The pubic peduncle is longer and more massive than the triangular ischial peduncle. The postacetabulum is almost rectangular, with a blunt posterior end. This differs from the situation in *Iteravis* (Zhou et al., 2014), but resembles the condition in adult *Archaeorhynchus* (Zhou and Zhang, 2006).

The **pubes** are incomplete, missing the distal ends (**Figures 3D**, **4C**,**D**). The left pubis seems to be exposed in lateral view, the right element in anterior view. The latter is still in contact with the left ilium, while the left pubis is slightly displaced posteriorly. The iliac peduncle of the left pubis shows a small anterior projection, and the peduncle's ventral margin bears a small embayment (**Figure 3D**). While such embayment is usually absent in

pygostylians, *Archaeopteryx* (Foth et al., 2014, Extended Data **Figure 2** and *Rahonavis* (Forster et al., 2020, Figure 31) display a similar morphology. In more basal theropods, this structure is described as an obturator notch (Rauhut, 2003). In the (sub-) adult *Archaeorhynchus* specimen IVPP V17075, the proximal end of the pubis is exposed in anteromedial view, showing no sign of an obturator notch. While the iliac peduncle of the pubis in this specimen is rather massive, the ischial peduncle is a thin, plate-like structure that fuses with the proximal end of the pubic shaft (Zhou et al., 2013). Beneath the right iliac peduncle of LNTU-WLMP-18, a small section of pubic shaft is broken away so that the underlying ischium is exposed. The pubic shafts are slender, and bowed both posteriorly and medially. Nothing can be said about the distal end of the pubic shaft, but based on the displacement of the left pubis, the distal ends must have been unfused, similar to the condition in (sub-)adult specimens of *Archaeorhynchus* (Zhou et al., 2013; Wang et al., 2016). However, the pubes probably contacted each other, as suggested by their curvature.

Both **ischia** are present (**Figures 4C,D**). The right ischium is complete, although the midshaft is interrupted by a crack in the slab. In the left ischium, the distal end is slightly broken. The ischium is shorter than the pubis, measuring about half the length of the ilium. The proximal end that forms the peduncles for the ilium and the pubis is short and broad, lacking the additional proximodorsal process present in many enantiornithines (e.g., Wang et al., 2010; Li et al., 2012; Hu et al., 2015; Wang and Zhou, 2017c) and more basal birds (e.g., Chiappe et al., 1999; Zhou and Zhang, 2002a; Zhou and Zhang, 2002b; Wellnhofer, 2009; Wang et al., 2018a). The shaft is simply straight, having a blunt distal end. Thus, the ischium resembles that of subadult specimens of *Archaeorhynchus* (Zhou et al., 2013) in possessing neither a strut-like proximodorsal process nor a gradual distal dorsal expansion along the shaft as in more advanced euornithines, like *Yixianornis* (Clarke et al., 2006), *Schizooura* (Zhou et al., 2012), *Iteravis* (Zhou et al., 2014) or *Dingavis* (O'Connor et al., 2016).

Hindlimbs

Both hindlimbs are present, and are more or less complete apart from the fragmentary preservation of the right foot. The left **femur** is still in articulation with the iliac portion of the acetabulum, lying perpendicular to the main body axis with the medial side visible (**Figure 2**). In contrast, the right femur lies parallel to the body axis, exposing the posterior surface. The femur is approximately as long as the humerus, whereas the humerus is longer than the femur in most other Pygostylia, including (sub-)adult specimens of *Archaeorhynchus* (Zhou and Zhang, 2002b; Zhou et al., 2012; Zhou et al., 2013; O'Connor et al., 2016). The femoral head is ball-shaped, and the neck is short (**Figure 4D**). The dorsal margin of the femur is convex from anterior view, and the greater trochanter is continuous with the lesser trochanter as in other pygostylians (Chiappe et al., 1999). The femoral shaft is relatively robust and straight, in contrast to most Paraves, where the shaft is curved (Norell and Makovicky, 1999; Zhou and Zhang, 2006; Clarke et al., 2006; O'Connor et al., 2011; Rauhut et al., 2018). In posterior view, the distal end of the femur is slightly expanded lateromedially with a small concavity interupting the ventral margin. In medial view the distal end appears rounded, with a minor posterior expansion. This expansion probably represents the remains of the distal condyles, but due to preservation not much more can be said about their morphology.

The right **tibia** lies medially to the corresponding femur, paralleling the body axis, and exhibiting its anterior surface. Approximately two-thirds of the tibia is preserved, with the distal end missing. Slightly disarticulated from the femur, the left tibia is complete, being slightly longer than the femur. The bone is exposed in posteromedial view. The proximal end of the tibia is lateromedially expanded. The shaft is straight, while the distal end does not show any distinctive features apart from a minor expansion (**Figure 2**). No **fibula** was identified. Fragmentary bone remains distal to the tibia might represent the **astragalus** (**Figures 4E,F**), in which cases the proximal tarsals would seem not to be fused with the tibia to form a tibiotarsus. This morphology resembles the condition seen in subadult specimens of *Archaeorhynchus* (Zhou and Zhang 2006; Zhou et al., 2013), but all three bones are fused to each other in adults (Wang et al., 2016).

Only the left **metatarsus**, which is exposed in anterior view, is completely preserved and still in articulation with the tibia. A short metatarsal I, whose shaft is triangular and expands into the distal condyle, articulates at the distal third of metatarsal II. As in subadult specimens of *Archaeorhynchus* (Zhou et al., 2013), metatarsals II–IV are unfused to each other along their entire lengths (**Figures 4E,F**), while adult specimens show proximal fusion among the metatarsal bones (Wang and Zhou 2017b). Proximally, all three metatarsals end at the same level. Metatarsal II is approximately as long and as wide as metatarsal IV, as in for instance *Longicrusavis* (O'Connor et al., 2010) or *Sapeornis* (Gao et al., 2012), while metatarsal III is the longest. In most *Archaeorhynchus* specimens, metatarsal II is shorter than metatarsal IV (Zhou and Zhang, 2006; Zhou et al., 2013), while in IVPP V20312, both metatarsal bones have almost the same length (Wang et al., 2016). Although the proximal and distal ends of metatarsal III are approximately as wide as those of the other metatarsals, the midshaft is slightly pinched. While the shaft of metatarsal III is almost straight, metatarsals II and IV are slightly curved medially and laterally direction, respectively. The distal trochleae of all three elements are slightly expanded. No remains of distal tarsals or metatarsal V can be identified.

The **pedal digits** of the left foot are preserved in articulation, with the fourth digit partly covered by the third (**Figure 4F**). Next to the right ulna, further phalanges are preserved in partial articulation. Based on their size they do not belong to the manus, and they are identified here as pedal phalanges of the right foot. The first phalanx of left digit I is longer than the corresponding metatarsus and ungual I. The phalanges of digits II to IV are relatively robust with the proximal elements being longer than the more distal ones. The pedal unguals are short and not strongly curved, with only small flexor tubercles at their proximal ends, as is typical for ground-dwelling birds (Hedrick et al., 2019).

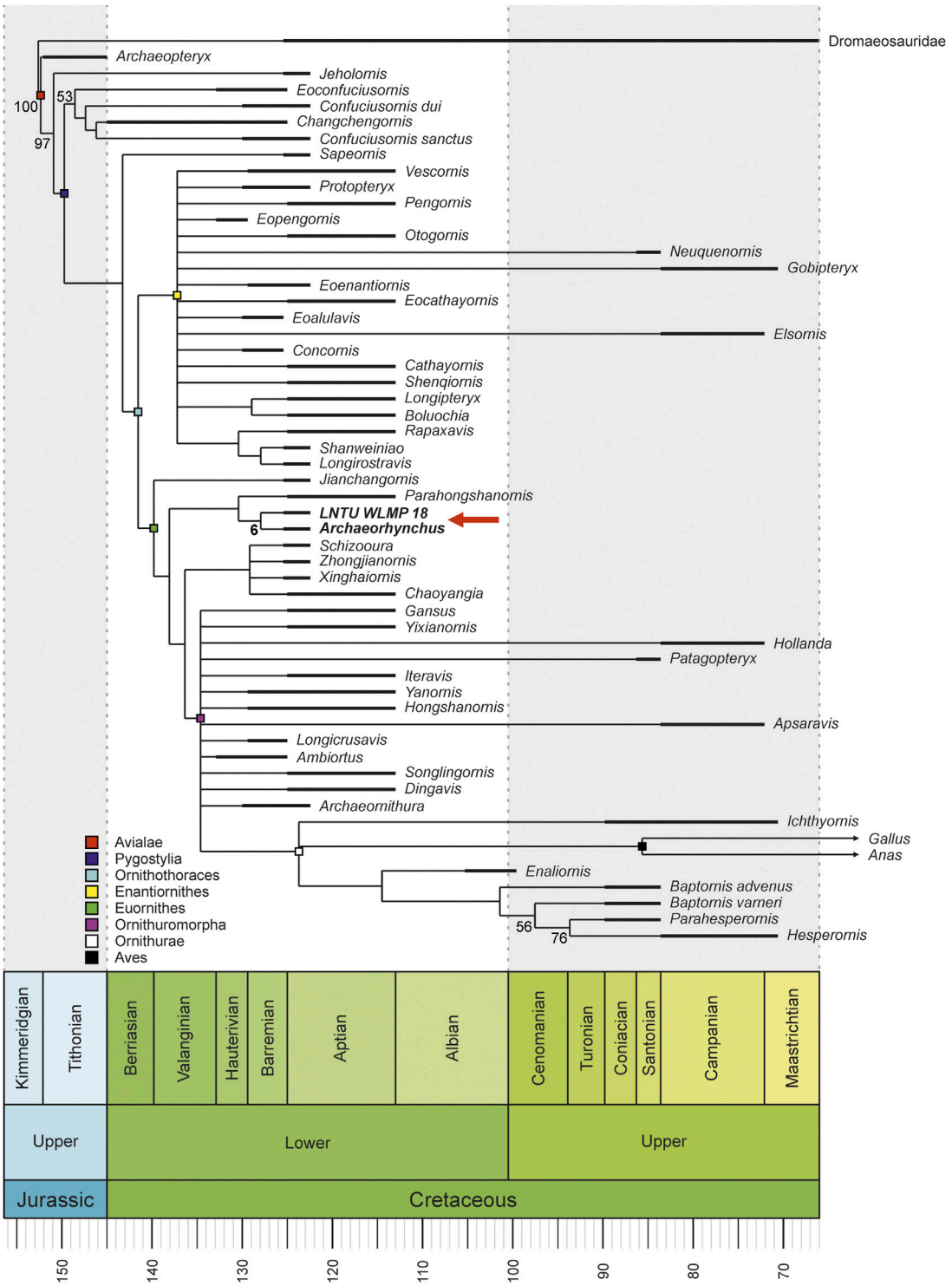

FIGURE 5 | Time-calibrated, reduced consensus tree (12,102 MPTs; length 900 steps) under equally weighted parsimony, showing the phylogenetic position of LNTU-WLMP-18 as sister taxon to *Archaeorhynchus*. Numbers at the nodes are bootstrap values for clades with more than 50% support. The support for the *Archaeorhynchus*–LNTU-WLMP-18 clade is also shown.

Feathers

The feathers are present as carbonized traces, but their preservation is rather poor (**Figure 2**). The plumage of the left wing provides the most detail. The primaries are long, and partly covered by the skull. Outlines of single feathers can be identified, but their actual morphology cannot be described. Dark patches

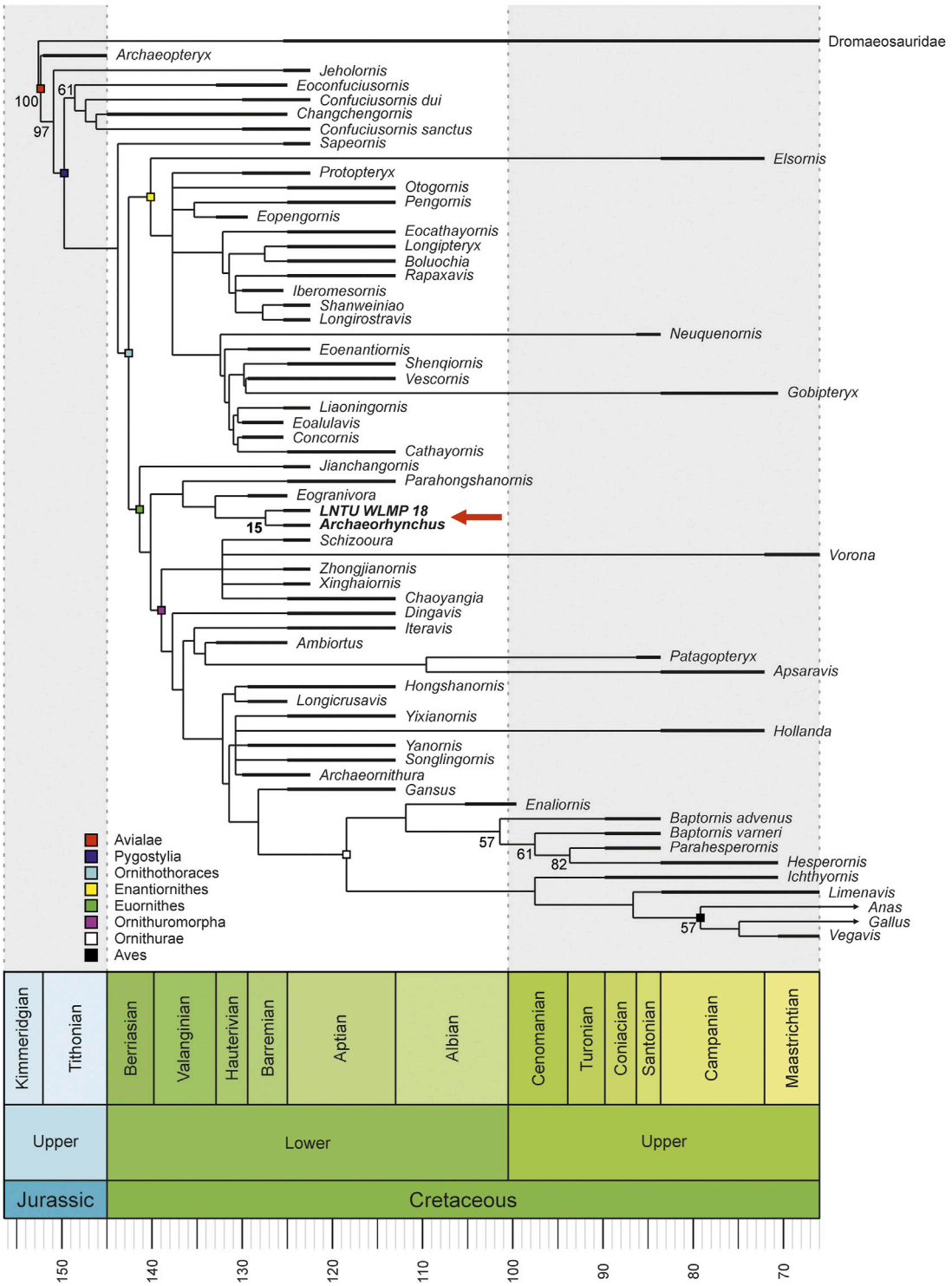

FIGURE 6 | Time-calibrated, strict consensus tree (125 MPTs; length 35.88411 steps) under implied-weighted parsimony, showing the phylogenetic position of LNTU-WLMP-18 as sister taxon to *Archaeorhynchus*. Numbers at the nodes are bootstrap values for clades with more than 50% support. The support for the *Archaeorhynchus*–LNTU-WLMP-18 clade is also shown.

situated posterior to the skull most likely represent remains of the secondaries. As preserved, they are approximately half as long as the primaries. The right wing plumage is also partly preserved. Small traces in the pelvic region may represent either body plumage or remains of the rectrices.

Intestinal Contents

A dark rope-like trace is preserved in the posterior portion of the torso, and probably represents the remains of gut contents (**Figure 2**). The structure is proportionally wider than intestinal tracts known from *Yanornis* (Zheng et al., 2014), but it is not possible to determine if the trace is formed by one intestinal loop or several ones that partially overlap each other. The supposed intestine contains small, round dark coaly and whitish clayey elements that measure between 1 and 2 mm in diameter (**Figures 4C,D**). They probably represent remains of ingested propagules of plants, e.g., round fruits, seeds, ovules, or parts thereof (see Mayr et al., 2020). In contrast to euornithine birds, including *Archaeorhynchus* (Zhou et al., 2004; Zhou and Zhang, 2006; Zhou et al., 2013; Chiappe et al., 2014; Zheng et al., 2018), no gastroliths, which could have helped processing ingested food, can be identified.

DISCUSSION

Taxonomic Identification of LNTU-WLMP-18

The phylogenetic analysis with equally weighted characters resulted in 12,102 trees with a length of 900 steps (**Figure 5**). Implied weighting resulted in 125 equally parsimonious trees with a length of 35.88411 steps (**Figure 6**). In both analyses, LNTU-WLMP-18 was identified as a member of the Euornithes based on the presence of a procoracoid process on the coracoid (char. 89; Wang et al., 2016). Further anatomical features supporting the placement of LNTU-WLMP-18 within euornithines are the rounded deltopectoral crest (O'Connor and Zelenkov, 2013) and coplanar proximal ends of metatarsals II–IV (Wang et al., 2016), and the absence of a tubercle on the dorsal face of metatarsal II (Chiappe, 2002). Within euornithines, LNTU-WLMP-18 was found to be the sister taxon to *Archaeorhynchus*, and this pairing formed a clade with *Parahongshanornis* and *Eogranivora*. The following characters support this clade: ratio between the diameters of the radial and ulnar shaft larger than 0.70 (char. 145), ischium without a proximodorsal process (char. 191), and metatarsal II approximately equal in distal extent to metatarsal IV (char. 236). Close affiliation to *Archaeorhynchus* is supported by an expanded sternolateral corner of the coracoid (char. 95), a humerus whose proximal and distal ends are expanded and nearly in the same plane (char. 121), an alular digit that does not extend distally beyond metacarpal II (char. 168), a weakly co-ossified tibia, calcaneum, and astragalus (char. 209), and a hallucal claw that is smaller than the other pedal claws (char. 243). Nevertheless, statistical support for this phylogeny is generally low, as the clade of LNTU-WLMP-18 and *Archaeorhynchus* is only supported by a bootstrap value of 15.

When compared with other edentulous euornithines from the Jehol Group, LNTU-WLMP-18 differs from *Eogranivora* in having a relatively short tibiotarsus compared to the femur (Zheng et al., 2018), and from *Dingavis, Schizooura, Xinghaiornis* and *Zhongjianornis* in having a relatively short tibiotarsus and metatarsus (Zhou et al., 2012; Wang et al., 2013a; Zhou et al., 2014; O'Connor et al., 2016; see also *Archaeornithura*; Wang et al., 2015; *Parahongshanornis,*; Li et al., 2011). LNTU-WLMP-18 differs from *Dingavis, Xinghaiornis* and *Zhongjianornis* in having a relatively short beak (Wang et al., 2013a; Zhou et al., 2014; O'Connor et al., 2016). Furthermore, LNTU-WLMP-18 is different from *Schizooura* and *Zhongjianornis* in having a small deltopectoral crest (Zhou et al., 2012; Zhou et al., 2014). Finally, LNTU-WLMP-18 is different from *Eogranivora* (Zheng et al., 2018), *Dingavis* (O'Connor et al., 2016) and *Archaeornithura* (Wang et al., 2015) in having a short metatarsal I and pedal digit I. LNTU-WLMP-18 lacks a dorsomedially oriented bluntly triangular process on the pubis (present in *Eogranivora*, Zheng et al., 2018), and a posterior intermediate expansion on the ischium (present in *Schizooura*, Zhou et al., 2012; *Archaeornithura,* Wang et al., 2015; and *Chaoyangia*, O'Connor and Zhou, 2013). Thus, based on the results of the phylogenetic analysis and comparisons with edentulous birds from the Jehol Group, we identify LNTU-WLMP-18 as a juvenile *Archaeorhynchus*, which would make it the ontogenetically youngest individual of this genus described so far based on its size and incompletely ossified bone surfaces (Zhou et al., 2013). Although the specimen is not sufficiently well preserved for all diagnostic characters of *Archaeorhynchus* to be evaluated (see emended diagnosis in Wang et al., 2016), the following characters support our identification: the upper and lower jaws are toothless; the dentary is spatulate; and the lateral margin of the coracoid is longer than the medial margin. The identification is further supported by similarities in manual and pelvic morphology (see above). Based on the femur length, LNTU-WLMP-18 is approximately 62.5 percent the size of the second smallest individual (IVPP V17091) and 54.5 percent the size of the largest specimen (IVPP V20312) (**Table 1**). Character differences with other specimens of *Archaeorhynchus* (listed below) are interpreted as ontogenetic variation and do not justify the establishment of a new taxon.

Ontogenetic Variation in *Archaeorhynchus*

Several ontogenetic studies on Mesozoic birds have been published so far, but are primarily restricted to Enantiornithes (Elzanowski, 1981; Sanz et al., 1997; Cambra-Moo et al., 2006; Chiappe et al., 2007; Kurochkin et al., 2013; Xing et al., 2017; Knoll et al., 2018; Xing et al., 2018; Kaye et al., 2019). The ontogeny of enantiornithine birds is characterized by relatively slow skeletal growth, but early onset of fledging that precedes skeletal maturation and indicates a highly precocial developmental mode (Elzanowski, 1981; Sanz et al., 1997;

Chiappe et al., 2007; Kurochkin et al., 2013; Knoll et al., 2018). However, interspecific comparison of osteogenesis in the sternum and pygostyle indicates great variation in the tempo of skeletal development, in relation to size, within Enantiornithes (Knoll et al., 2018). Knowledge of ontogenetic trends among Early Cretaceous euornithines was previously based solely on one adult and four subadult specimens of *Archaeorhynchus* (Zhou and Zhang, 2006; Zhou et al., 2013; Wang and Zhou 2017b; Wang et al., 2018). As LNTU-WLMP-18 is the first known juvenile euornithine that can be assigned to a particular genus, the specimen helps to improve our knowledge of early ontogeny not only in *Archaeorhynchus,* but among early euornithines in general.

The bone histology of *Archaeorhynchus* reveals relatively slow growth, with more than three years needed to reach skeletal maturity (Wang and Zhou, 2017b). This is different from the growth patterns found in other Early Cretaceous euornithines, like *Iteravis* (O'Connor et al., 2015) and *Yanornis* (J. Wang et al., 2019), and from the growth of extant birds (Ricklefs 1968; Scheyer et al., 2010), but similar to Enantiornithes (Chinsamy et al., 1994; O'Connor et al., 2014). Previous studies have demonstrated that *Archaeorhynchus* shows distinct morphological changes even in its late ontogeny. The sternum of adult individuals differs from that of subadults in being proportionally longer, and in having fan-shaped zyphoid processes and a proportionally more elongated xiphoid process at the posterior end (Wang and Zhou, 2017b). This indicates that the process of sternal ossification in *Archaeorhynchus* was not completed until an advanced postnatal developmental stage. *Archaeorhynchus* also shows late ontogenetic fusion of the pygostyle, the carpometacarpus, the tibiotarsus and the proximal end of the tarsometatarsus (Zhou et al., 2013; Wang and Zhou, 2017b). This differs from the situation in extant birds, in which fusion of bones happens relatively early during postnatal development (e.g., Schepelmann, 1990). This precocious fusion process is probably driven by the accelerated growth pattern of extant birds (Starck and Ricklefs, 1998a; Scheyer et al., 2010). Unfortunately, the new specimen cannot provide new information on the ossification pattern of the sternum or the pygostyle, as these elements are not preserved. As in subadult specimens of this genus, the carpometacarpus, tibiotarsus and tarsometatarsus are not yet developed due to lack of fusion (see above). Similarly, the sacral vertebrae of LNTU-WLMP-18 are still unfused with each other and the ilia. However, the first four of the seven sacrals of the subadult specimen IVPP V17075 form a synsacrum (Zhou et al., 2013), while in the holotype IVPP V14287, which is only slightly bigger than IVPP V17075, all seven sacrals are fused into a synsacrum (Zhou and Zhang, 2006). This indicates that the sacral region of *Archaeorhynchus* shows an earlier onset of fusion than the distal limb elements, as is also the case in Enantiornithes (Hu and O'Connor 2017).

Although the skulls of the various known specimens of *Archaeorhynchus* are incomplete or badly crushed, the premaxilla (including the nasal process) is estimated to account for a slightly smaller proportion of total skull length in LNTU-WLMP-18 (c. 36 percent) than in IVPP V17075 (c. 42 percent). Although these measurements have to be interpreted with caution, the proportional differences, if correct, could indicate the presence of a relatively shorter beak in the younger individual, as is typical for juveniles birds in general (e.g., Sosa and Hospitaleche, 2018; Piro and Hospitaleche, 2019). Differences in limb proportions can be more reliably identified. The forelimbs of LNTU-WLMP-18 are significantly shorter relative to the hindlimbs (*t*-value: 90.08; *p*-value: < 0.0001) than in the other known individuals, which all have almost identical proportions (**Figure 7A**). Relative to humeral length, the ulna of LNTU-WLMP-18 is significantly shorter than in other individuals (*t*-value: 4.23; *p*-value: 0.024), while metacarpals I and II are significantly longer (Mc-I: *t*-value: −7.13; *p*-value: 0.006; Mc-II: *t*-value: −7.78; *p*-value: 0.004). While the length ratio between the tibia and metatarsal III is more or less similar in all *Archaeorhynchus* individuals (*t*-value: 2.64; *p*-value: 0.077), the femur of LNTU-WLMP-18 is unsually long in comparision to the tibia (*t*-value: 16.26; *p*-value: <0.001) and metatarsal III (*t*-value: 4.64; *p*-value: 0.019). These results indicate 1) that the forelimbs of *Archaeorhynchus* increased in length during ontogeny, and b) that proportions within the forelimb change more during ontogeny than proportions within the hindlimb (**Table 2**). This is similar to the situation in *Archaeopteryx* (Wellnhofer, 1974), but different to that in the enantiornithine hatchlings of *Gobipipus* and *Gobipteryx,* in which the forelimbs are already longer than the hindlimbs (Elzanowski, 1981; Kurochkin et al., 2013). However, in other Enantiornithes the ratios are more similar to LNTU-WLMP-18 (Chiappe et al., 2007). As in early juvenile Enantiornithes, LNTU-WLMP-18 possesses straight scapulae and femora (Elzanowski, 1981; Chiappe et al., 2007; Kurochkin et al., 2013), while in subadult and adult individuals of *Archaeorhynchus* these elements are curved (Zhou and Zhang, 2006; Zhou et al., 2013; Wang et al., 2016).

The rib morphology of LNTU-WLMP-18 indicates that uncinate processes also developed later in ontogeny. These processes are present in the holotype of *Archaeorhynchus* (Zhou and Zhang, 2006), but are described as being absent in subadult individuals (Zhou et al., 2013). However, Zhou et al. (2013) mention the presence of short and robust gastralia in IVPP V17075 and IVPP V14287. In both specimens, these bones are associated with the thoracic ribs, and in IVPP V17075, the elements of the left side are even aligned with each other in an anteroposteriorly directed pattern. Therefore, we speculate that these short, robust elements are in fact uncinate processes, indicating the presence of these structures in subadult individuals of this genus. Furthermore, the morphology of the humerus reveals that the deltopectoral crest was weakly developed in early juveniles, but grew more prominent during ontogeny. Finally, LNTU-WLMP-18 differs from other *Archaeorhynchus* specimens in having a ventral embayment between the ischial peduncle and the proximal end of the pubic shaft, which resembles the obturator notch in non-pygostylian theropods (Rauhut, 2003). In (sub)adult individuals the plate-like ischial peduncle is continuous with the proximal end of the pubic shaft (Zhou et al., 2013). Due to the preservation, we cannot fully rule out the possibility that this fossa results from breakage. If this

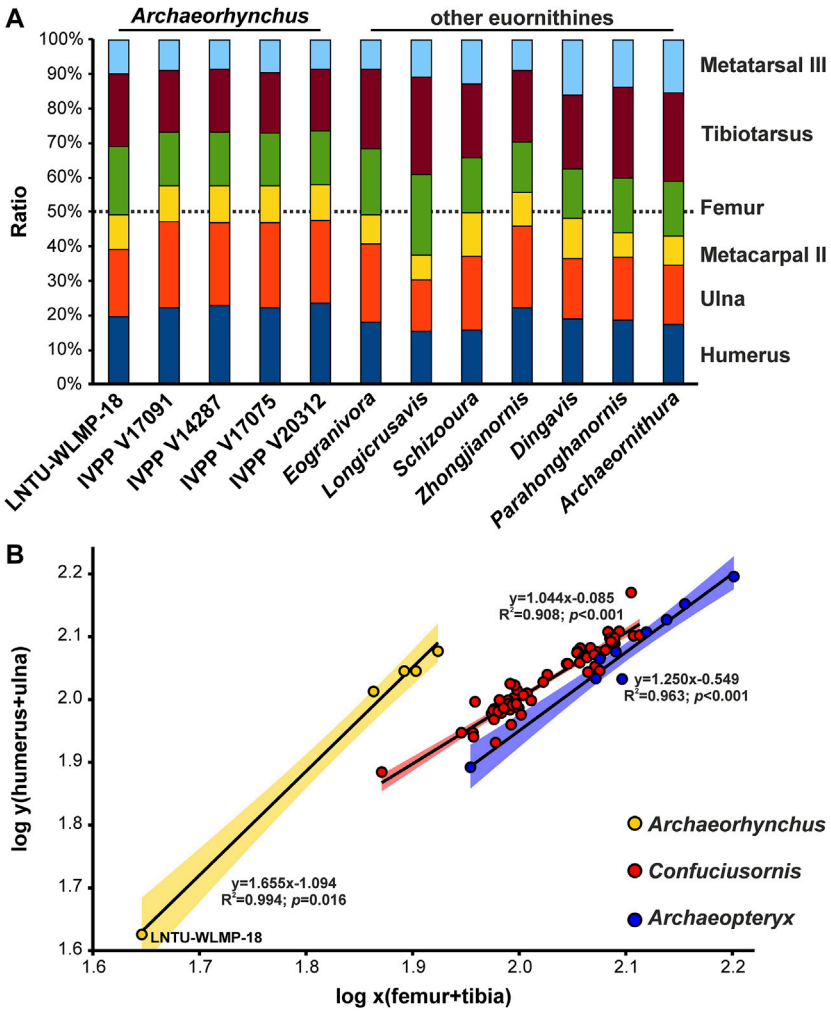

FIGURE 7 | Limb proportions of Early Cretaceous Euornithines. **(A)** Histogram comparing the limb proportions of LNTU-WLMP-18 with those of different *Archaeorhynchus* specimens and other euornithine species. **(B)** Ordinary linear regression between log-transformed forelimb and hindlimb element lengths comparing *Archaeorhynchus* (including LNTU-WLMP-18), *Confuciusornis* (see Chiappe et al., 2008) and *Archaeopteryx* (see Rauhut et al., 2018).

structure is genuine, this would be an ontogenetic character change that recapitulated a corresponding character change during evolution. However, further early juvenile ornithothoracine bird specimens from the Early Cretaceous will be needed to evaluate this hypothesis.

Examining the ontogenetic trajectory of ratio between forelimb and hindlimb length, the slope for *Archaeorhynchus* is significantly different from that for *Archaeopteryx* (*F*-value: 7.315; *p*-value: 0.022) or *Confuciusornis* (*F*-value: 25.970; *p*-value: <0.001), showing strong positive ontogenetic allometry (slope: 1.655; R^2: 0.994; *p*-value: 0.016) of the forelimb relative to the hindlimb. *Archaeopteryx* shows also positive allometry (slope: 1.250; R^2: 0.963; *p*-value: <0.001), while in *Confuciusornis* the forelimb is almost isometric to the hindlimb (slope: 1.044; R^2: 0.908; *p*-value: <0.001). Nevertheless, the trajectory slopes of *Archaeopteryx* and *Confuciusornis* are statistically indistinguishable (*F*-value: 1.950; *p*-value: 0.167) (**Figure 7B**).

Despite the small body size and weak degree of bone fusion, the extensive wing plumage of LNTU-WLMP-18 indicates that the specimen was already fledged, implying an early onset of flight ability in the ontogeny of basal euornithines, as in Enantiornithes and extant birds (Carrier and Auriemma, 1992). In contrast to extant birds, fledging and skeletal maturity were not ontogenetically synchronized in basal Euornithes and Enantiornithes. In fact, based on femoral length, LNTU-WLMP-18 had no more than 22% of the body mass of IVPP V14287 (see Field et al., 2013 for body mass estimation) (**Figure 8**). Thus, the early onset of fledging in early Ornithothoraces did not interfere with their ancestral growth pattern. Whether *Archaeorhynchus* was also precocial cannot be answered with absolute certainty, as this requires the discovery of earlier ontogenetic stages close to hatching. However, the relatively long hindlimbs, the short first pedal phalanx and the generally slight curvature of the pedal claws indicate that LNTU-

FIGURE 8 | Reconstruction of *Archaeorhynchus* growth stages, with the new juvenile LNTU-WLMP-18 on the left. Note the nearly adult-like proportions of the wing bones and primary feathers, even though the trunk is only about half as long as in an adult. Subadult stage in the center reconstructed from IVPP V14287, 17,075, 17,091, and STM7-11 (Zhou and Zhang, 2006; Zhou et al., 2013; Wang et al., 2018b; respectively), with still unfused metacarpals. Adult stage on the right reflecting IVPP V20312 (Wang et al., 2016), with plumage inferred from subadults. Scale bar in cm.

WLMP-18 was ground-dwelling rather than arboreal. A similar mode of life is also suggested for (sub-)adult individuals of *Archaeorhynchus* (Zhou and Zhang, 2006; Zhou et al., 2013; Wang et al., 2016) and other Early Cretaceous ornithuromorph euornithines (Zhou and Zhang, 2005; Bell and Chiappe, 2011; Wang et al., 2016). Together with relatively early onset of fledging, a precocial ontogeny is more likely than an altricial one (Starck and Ricklefs, 1998b). Finally, the fossilized intestinal remains indicate that early juveniles of *Archaeorhynchus* fed on plant propagules, most likely seeds or seed-containing fruits (Mayr et al., 2020). Studies on modern seed-eating birds indicate that individuals at different ontogenetic stages may prefer seeds of differing sizes (Kear, 1962; Newton, 1967; Díaz, 1996). The fact that LNTU-WLMP-18 lacks gastroliths, in contrast to larger specimens of *Archaeorhynchus* (Zhou and Zhang, 2006; Zhou et al., 2013; Wang et al., 2016), might indicate a dietary shift through ontogeny. Being seed-eating and ground-dwelling, *Archaeorhynchus* differs in its ecological adaptations from most Enantiornithes, but filled an ecological niche that may have allowed basal crown birds to survive the K-Pg mass extinction (Field et al., 2018).

DATA AVAILABILITY STATEMENT

The original contributions presented in the study are included in the article/**Supplementary Material**, further inquiries can be directed to the corresponding author.

ETHICS STATEMENT

Ethical review and approval was not required for the animal study because the specimen studied is a fossil of an animal that died 125 Myrs ago.

AUTHOR CONTRIBUTIONS

FC, WS, SF, LY, and YR designed the project. FC, WS, SF, LY and YR performed the research. FC, WS, and SF wrote the manuscript. All authors contributed to the article and approved the submitted version.

FUNDING

This research was supported by the Swiss National Science Foundation (PZ00P2_174040 to CF), the German Science Foundation (FO 1005/2-1 to CF) and the Liaoning Technical University of Fuxin.

ACKNOWLEDGMENTS

Michael Völker and Raimund Albersdörfer (both Dinosaur Museum Altmühltal, Denkendorf, Germany) are thanked for sponsoring the research trip (to FS). We are furthermore grateful to Liang Bing and Han Jun for hosting us at the Liaoning Technical University (Fuxin, China). We further thank Sebastian Apesteguia and Jingmai O'Connor for their critical reviews and Walter Joyce and Corwin Sullivan for proofreading. Finally, we thank the editors Jingmai O'Connor, Corwin Sullivan and Daniel Field for the invitation to contribute to the article collection "Early Avian Evolution" in Frontiers in Earth Science.

SUPPLEMENTARY MATERIAL

The Supplementary Material for this article can be found online at: https://www.frontiersin.org/articles/10.3389/feart.2021.604520/full#supplementary-material.

REFERENCES

Baumel, J. J., and Witmer, L. M. (1993). "Osteologia," in *Handbook of avian anatomy*. Editors J. J. Baumel, A. S. King, J. E. Breazile, H. E. Evans, and J. C. Vanden Berge (Cambridge, MA: Nuttall Ornithological Club), 45–132.

Bell, A., and Chiappe, L. M. (2011). Statistical approach for inferring ecology of Mesozoic birds. *J. Syst. Palaeontology* 9, 119–133. doi:10.1080/14772019.2010.525536

Benson, R. B. J., Campione, N. E., Carrano, M. T., Mannion, P. D., Sullivan, C., Upchurch, P., et al. (2014). Rates of dinosaur body mass evolution indicate 170 million years of sustained ecological innovation on the avian stem lineage. *Plos Biol.* 12, e1001853. doi:10.1371/journal.pbio.1001853

Benton, M. J., Zhou, Z., Orr, P. J., Zhang, F., and Kearns, S. L. (2008). The remarkable fossils from the Early Cretaceous Jehol Biota of China and how they have changed our knowledge of Mesozoic life. *Proc. Geol. Assoc.* 119, 209–228. doi:10.1111/j.1525-142x.2011.00478.x

Bever, G. S., Gauthier, J. A., and Wagner, G. P. (2011). Finding the frame shift: digit loss, developmental variability, and the origin of the avian hand. *Evol. Dev.* 13, 269–279. doi:10.1111/j.1525-142x.2011.00478.x

Bhullar, B.-A. S., Marugán-Lobón, J., Racimo, F., Bever, G. S., Rowe, T. B., Norell, M. A., et al. (2012). Birds have paedomorphic dinosaur skulls. *Nature* 487, 223–226. doi:10.1038/nature11146

Brown, R. H. J. (1963). The flight of birds. *Biol. Rev.* 38, 460–489. doi:10.1111/j.1469-185x.1963.tb00790.x

Burke, A. C., and Feduccia, A. (1997). Developmental patterns and the identification of homologies in the avian hand. *Science* 278, 666–668. doi:10.1126/science.278.5338.666

Cambra-Moo, O., Chamero, B., Marugán-Lobón, J., Delclós, X., Poyato-Ariza, F. J., and Buscalioni, A. D. (2006). Estimating the ontogenetic status of an enantiornithine bird from the lower barremian of el montsec, central pyrenees, Spain. *Estud. Geológicos* 62, 241–248. doi:10.3989/egeol.0662123

Cao, H., and He, W. (2019). Correlation of carbon isotope stratigraphy and paleoenvironmental conditions in the Cretaceous Jehol Group, northeastern China. *Int. Geology. Rev.* 62, 113–128. doi:10.1080/00206814.2019.1681303

Carrier, D. R., and Auriemma, J. (1992). A developmental constraint on the fledging time of birds. *Biol. J. Linn. Soc.* 47, 61–77. doi:10.1111/j.1095-8312.1992.tb00656.x

Chiappe, L. M. (2002). "Basal bird phylogeny: problems and solutions," in *Mesozoic birds: above the heads of dinosaurs*. Editors L. M. Chiappe and L. M. Witmer (Berkeley, CA: University of California Press), 448–472.

Chiappe, L. M., Di, L., Serrano, F. J., Yuguang, Z., and Meng, Q. (2020). Anatomy and flight performance of the early enantiornithine bird protopteryx fengningensis : information from new specimens of the early cretaceous huajiying formation of China. *Anat. Rec.* 303, 716–731. doi:10.1002/ar.24322

Chiappe, L. M., and Göhlich, U. B. (2010). Anatomy of *Juravenator starki* (theropoda: Coelurosauria) from the late jurassic of Germany. *N. Jb. Geol. Paläont. Abh.* 258, 257–296. doi:10.1127/0077-7749/2010/0125

Chiappe, L. M., Ji, S., Ji, Q., and Norell, M. A. (1999). Anatomy and systematics of the Confuciusornithidae (theropoda: aves) from the late mesozoic of northeastern China. *Bull. Am. Mus. Nat. Hist.* 242, 1–89.

Chiappe, L. M., Marugán-Lobón, J., Ji, S. a., and Zhou, Z. (2008). Life history of a basal bird: morphometrics of the Early Cretaceous *Confuciusornis*. *Biol. Lett.* 4, 719–723. doi:10.1098/rsbl.2008.0409

Chiappe, L. M., and Meng, Q. (2016). *Birds of stone*. Baltimore, MD: Johns Hopkins University Press.

Chiappe, L. M., Shu'An, J., and Qiang, J. (2007). Juvenile birds from the Early Cretaceous of China: implications for enantiornithine ontogeny. *Am. Mus. Novitates* 3594, 1–49. doi:10.1206/0003-0082(2007)3594[1:jbftec]2.0.co;2

Chiappe, L. M., Zhao, B., O'Connor, J. K., Chunling, G., Wang, X., Habib, M., et al. (2014). A new specimen of the Early Cretaceous birdHongshanornis longicresta: insights into the aerodynamics and diet of a basal ornithuromorph. *PeerJ* 2, e234. doi:10.7717/peerj.234

Chinsamy, A., Chiappe, L. M., and Dodson, P. (1994). Growth rings in Mesozoic birds. *Nature* 368, 196–197. doi:10.1038/368196a0

Clarke, J. A., Zhou, Z., and Zhang, F. (2006). Insight into the evolution of avian flight from a new clade of Early Cretaceous ornithurines from China and the morphology of *Yixianornis grabaui*. *J. Anat.* 208, 287–308. doi:10.1111/j.1469-7580.2006.00534.x

Dal Sasso, C., and Maganuco, S. (2011). *Scipionyx samniticus* (theropoda: compsognathidae) from the lower cretaceous of Italy. Osteology, ontogenetic assessment, phylogeny, soft tissue anatomy, taphonomy and paleobiology. *Hist. Biol.* 37, 1–281.

Díaz, M. (1996). Food choice by seed-eating birds in relation to seed chemistry. *Comp. Biochem. Physiol. A: Physiol.* 113, 239–246. doi:10.1016/0300-9629(95)02093-4

Elzanowski, A. (1981). Embryonic bird skeletons from the late cretaceous of Mongolia. *Palaeontol. Pol.* 42, 147–179.

Feduccia, A., Lingham-Soliar, T., and Hinchliffe, J. R. (2005). Do feathered dinosaurs exist? Testing the hypothesis on neontological and paleontological evidence. *J. Morphol.* 266, 125–166. doi:10.1002/jmor.10382

Field, D. J., Bercovici, A., Berv, J. S., Dunn, R., Fastovsky, D. E., Lyson, T. R., et al. (2018). Early evolution of modern birds structured by global forest collapse at the End-Cretaceous mass extinction. *Curr. Biol.* 28, P1825–P1831. doi:10.1016/j.cub.2018.04.062

Field, D. J., Lynner, C., Brown, C., and Darroch, S. A. F. (2013). Skeletal correlates for body mass estimation in modern and fossil flying birds. *PLoS One* 8, e82000. doi:10.1371/journal.pone.0082000

Forster, C. A., O'Connor, P. M., Chiappe, L. M., and Turner, A. H. (2020). The osteology of the Late Cretaceous paravian *Rahonavis ostromi* from Madagascar. *Palaeontol. Electron.* 23, 147–176. doi:10.26879/793

Foth, C., Haug, C., Haug, J. T., Tischlinger, H., and Rauhut, O. W. M. (2020). "Two of a feather: a comparison of the preserved integument in the juvenile theropod dinosaurs *Sciurumimus* and *Juravenator* from the Kimmeridgian Torleite Formation of southern Germany," in *The evolution of feathers*. Editors C. Foth and O. W. M. Rauhut (Basingstoke, United Kingdom: Springer Nature), 79–101.

Foth, C., Hedrick, B. P., and Ezcurra, M. D. (2016). Cranial ontogenetic variation in early saurischians and the role of heterochrony in the diversification of predatory dinosaurs. *PeerJ* 4, e1589. doi:10.7717/peerj.1589

Foth, C., Tischlinger, H., and Rauhut, O. W. M. (2014). New specimen of *Archaeopteryx* provides insights into the evolution of pennaceous feathers. *Nature* 511, 79–82. doi:10.1038/nature13467

Gao, C., Chiappe, L. M., Zhang, F., Pomeroy, D. L., Shen, C., Chinsamy, A., et al. (2012). A subadult specimen of the Early Cretaceous birdSapeornis chaoyangensisand a taxonomic reassessment of sapeornithids. *J. Vertebr. Paleontol.* 32, 1103–1112. doi:10.1080/02724634.2012.693865

Goloboff, P. A., and Catalano, S. A. (2016). TNT version 1.5, including a full implementation of phylogenetic morphometrics. *Cladistics* 32, 221–238. doi:10.1111/cla.12160

Goloboff, P. A., Farris, J. S., and Nixon, K. C. (2008). TNT, a free program for phylogenetic analysis. *Cladistics* 24, 774–786. doi:10.1111/j.1096-0031.2008.00217.x

Goloboff, P. A., Torres, A., and Arias, J. S. (2018). Weighted parsimony outperforms other methods of phylogenetic inference under models appropriate for morphology. *Cladistics* 34, 407–437. doi:10.1111/cla.12205

Guinard, G. (2015). Limusaurus inextricabilis(Theropoda: ceratosauria) gives a hand to evolutionary teratology: a complementary view on avian manual digits identities. *Zool. J. Linn. Soc.* 176, 674–685. doi:10.1111/zoj.12329

Hammer, O., and Harper, D. A. T. (2006). *Paleontological data analysis*. Malden, MA: Blackwell Publishing.

Hammer, O., Harper, D. A. T., and Ryan, P. D. (2001). *PAST*: paleontological statistics software package for education and data analysis. *Palaeontol. Electron.* 4, 9.

Haug, J. T., and Haug, C. (2011). Fossilien unter langwelligem Licht: grün-Orange-Fluoreszenz an makroskopischen Objekten. *Archaeopteryx* 29, 20–23.

Haug, J. T., Haug, C., Kutschera, V., Mayer, G., Maas, A., Liebau, S., et al. (2011). Autofluorescence imaging, an excellent tool for comparative morphology. *J. Microsc.* 244, 259–272. doi:10.1111/j.1365-2818.2011.03534.x

Hedrick, B. P., Cordero, S. A., Zanno, L. E., Noto, C., and Dodson, P. (2019). Quantifying shape and ecology in avian pedal claws: the relationship between the bony core and keratinous sheath. *Ecol. Evol.* 9, 11545–11556. doi:10.1002/ece3.5507

Herzog, K. (1968). *Anatomie und Flugbiologie der Vögel*. Jena, Germany: Gustav Fischer Verlag.

Hinchliffe, J. R., and Hecht, M. K. (1984). Homology of the bird wing skeleton. *Evol. Biol.* 18, 21–39. doi:10.1007/978-1-4615-6977-0_2

Hone, D. W. E., Farke, A. A., and Wedel, M. J. (2016). Ontogeny and the fossil record: what, if anything, is an adult dinosaur? *Biol. Lett.* 12, 20150947. doi:10.1098/rsbl.2015.0947

Hu, D., Liu, Y., Li, J., Xu, X., and Hou, L. (2015). *Yuanjiawaornis viriosus*, gen. et sp. nov., a large enantiornithine bird from the Lower Cretaceous of western Liaoning, China. *Cretaceous Res.* 55, 210–219. doi:10.1016/j.cretres.2015.02.013

Hu, H., and O'Connor, J. K. (2017). First species of Enantiornithes from Sihedang elucidates skeletal development in Early Cretaceous enantiornithines. *J. Syst. Palaeontology* 15, 909–926. doi:10.1080/14772019.2016.1246111

Kaye, T. G., Pittman, M., Marugán-Lobón, J., Martín-Abad, H., Sanz, J. L., and Buscalioni, A. D. (2019). Fully fledged enantiornithine hatchling revealed by Laser-Stimulated Fluorescence supports precocial nesting behavior. *Sci. Rep.* 9, 5006. doi:10.1038/s41598-019-41423-7

Kear, J. (1962). Food selection in finches with special reference to the interspecific differences. *J. Zool.* 138, 163–204.doi:10.1111/j.1469-7998.1962.tb05694.x

Knoll, F., Chiappe, L. M., Sanchez, S., Garwood, R. J., Edwards, N. P., Wogelius, R. A., et al. (2018). A diminutive perinate European Enantiornithes reveals an asynchronous ossification pattern in early birds. *Nat. Commun.* 9, 937. doi:10.1038/s41467-018-03295-9

Kurochkin, E. N., Chatterjee, S., and Mikhailov, K. E. (2013). An embryonic enantiornithine bird and associated eggs from the Cretaceous of Mongolia. *Paleontol. J.* 47, 1252–1269. doi:10.1134/s0031030113110087

Li, L., Jinqi, W., Xi, Z., and Shilin, H. (2012). A new enantiornithine bird from the lower cretaceous Jiufotang Formation in jinzhou area, western liaoning province, China. *Acta Geol. Sin.* 86, 1039–1044. doi:10.1111/j.1755-6724.2012.00729.x

Li, L., Wang, J., and Hou, S. (2011). A new ornithurine bird (hongshanornithidae) from the juifotang formation of chaoyang, liaoning, China. *Vertebr. Palasiat.* 49, 195–200.

Liu, Y.-Q., Kuang, H.-W., Jiang, X.-J., Peng, N., Xu, H., and Sun, H.-Y. (2012). Timing of the earliest known feathered dinosaurs and transitional pterosaurs older than the Jehol Biota. *Palaeogeogr. Palaeoclimatol. Palaeoecol.* 323-325, 1–12. doi:10.1016/j.palaeo.2012.01.017

Mayr, G. (2017). *Avian evolution*. Chichester, United Kingdom: John Wiley.

Mayr, G., Kaye, T. G., Pittman, M., Saitta, E. T., and Pott, C. (2020). Reanalysis of putative ovarian follicles suggests that Early Cretaceous birds were feeding not breeding. *Sci. Rep.* 10, 19035. doi:10.1038/s41598-020-76078-2

Newton, I. (1967). The adaptive radiation and feeding ecology of some British finches. *Ibis* 109, 33–96. doi:10.1111/j.1474-919X.1967.tb00005.x

Norell, M. A., and Makovicky, P. J. (1999). Important features of the dromaeosaurid skeleton II: information from newly collected specimens of *Velociraptor mongoliensis*. *Am. Mus. Novit.* 3282, 1–45.

O'Connor, J. K. (2020). The plumage of basal birds. *The evolution of feathers* Editors C. Foth and O. W. M. Rauhut (Cham. Springer Nature), 147–172.

O'Connor, J. K., and Chiappe, L. M. (2011). A revision of enantiornithine (Aves: Ornithothoraces) skull morphology. *J. Syst. Palaeontol.* 9, 135–157. doi:10.1080/14772019.2010.526639

O'Connor, J. K., Chiappe, L. M., Gao, C., and Zhao, B. (2011). Anatomy of the early cretaceous enantiornithine bird *Rapaxavis pani*. *Acta Palaeontol. Pol.* 56, 463–475. doi:10.4202/app.2010.0047

O'Connor, J. K., Gao, K., and Chiappe, L. M. (2010). A new ornithuromorph (Aves: Ornithothoraces) bird from the Jehol Group indicative of higher-level diversity. *J. Vertebr. Paleontol.* 30, 311–321. doi:10.1080/02724631003617498

O'Connor, J. K., Wang, M., and Hu, H. (2016). A new ornithuromorph (Aves) with an elongate rostrum from the Jehol Biota, and the early evolution of rostralization in birds. *J. Syst. Palaeontol.* 14, 939–948. doi:10.1080/14772019.2015.1129518

O'Connor, J. K., Wang, M., Zheng, X., Wang, X., and Zhou, Z. (2014). The histology of two female Early Cretaceous birds. *Vertebr. Palasiat.* 52, 112–128.

O'Connor, J. K., Wang, M., Zhou, S., and Zhou, Z. (2015). Osteohistology of the lower cretaceous yixian formation ornithuromorph (aves) *Iteravis huchzermeyeri*. *Palaeontol. Electron.* 18, 1–11. doi:10.26879/520

O'Connor, J. K., and Zelenkov, N. V. (2013). The phylogenetic position of *Ambiortus*: comparison with other Mesozoic birds from Asia. *Paleontol. J.* 47, 1270–1281. doi:10.1134/S0031030113110063

O'Connor, J. K., and Zhou, Z. (2013). A redescription of *Chaoyangia beishanensis* (Aves) and a comprehensive phylogeny of Mesozoic birds. *J. Syst. Palaeontol.* 11, 889–906. doi:10.1080/14772019.2012.690455

Piro, A., and Acosta Hospitaleche, C. (2019). Skull morphology and ontogenetic variation of the southern giant petrel *Macronectes giganteus* (aves: procellariiformes). *Polar Biol.* 42, 27–45. doi:10.1007/s00300-018-2397-z

Plateau, O., and Foth, C. (2020). Birds have peramorphic skulls, too: anatomical network analyses reveal oppositional heterochronies in avian skull evolution. *Commun. Biol.* 3, 195. doi:10.1038/s42003-020-0914-4

Rauhut, O. W. M., Foth, C., Tischlinger, H., and Norell, M. A. (2012). Exceptionally preserved juvenile megalosauroid theropod dinosaur with filamentous integument from the Late Jurassic of Germany. *Proc. Natl. Acad. Sci.* 109, 11746–11751. doi:10.1073/pnas.1203238109

Rauhut, O. W. M., Foth, C., and Tischlinger, H. (2018). The oldest *Archaeopteryx* (theropoda: avialiae): a new specimen from the kimmeridgian/tithonian boundary of schamhaupten, bavaria. *PeerJ* 6, e4191. doi:10.7717/peerj.4191

Rauhut, O. W. M. (2003). The interrelationships and evolution of basal theropod dinosaurs. *Spec. Pap. Palaeontol.* 69, 1–213.

Ricklefs, R. E. (1968). Patterns of growth in birds. *Ibis* 110, 419–451. doi:10.1111/j.1474-919X.1968.tb00058.x

Sanz, J. L., Chamero, B., Chiappe, L. M., Marugán-Lobón, J., O'Connor, J. K., Ortega, F., et al. (2016). "Aves," in *Las hoyas. A cretaceous wetland*. Editors F. J. Poyato-Ariza and A. D. Buscalioni (Munich, Germany: Verlag Dr. Friedrich Pfeil), 183–189.

Sanz, J. L., Chiappe, L. M., Pérez-Moreno, B. P., Moratalla, J. J., Hernández-Carrasquilla, F., Buscalioni, A. D., et al. (1997). A nestling bird from the Lower Cretaceous of Spain: implications for avian skull and neck evolution. *Science* 276, 1543–1546. doi:10.1126/science.276.5318.1543

Sanz, J. L., Pérez-Moreno, B. P., Chiappe, L. M., and Buscalioni, A. D. (2002). "The birds from the lower cretaceous of las hoyas (province of cuenca, Spain)," in *In* mesozoic birds: Above the Heads of dinosaurs. Editors L. M. Chiappe and L. M. Witmer (Berkeley, CA: University of California Press), 209–267.

Schepelmann, K. (1990). Erythropoietic bone marrow in the pigeon: development of its distribution and volume during growth and pneumatization of bones. *J. Morphol.* 203, 21–34. doi:10.1002/jmor.1052030104

Scheyer, T. M., Klein, N., and Sander, P. M. (2010). Developmental palaeontology of Reptilia as revealed by histological studies. *Semin. Cel Developmental Biol.* 21, 462–470. doi:10.1016/j.semcdb.2009.11.005

Sereno, P. C., Rao, C., and Li, J. (2002). "*Sinornis santensis* (aves: Enantiornithes) from the early cretaceous of northeastern China," in *Mesozoic birds: Above the heads of Dinosaurs*. Editors L. M. Chiappe and L. M. Witmer (Berkeley, CA: University of California Press), 184–208.

Sosa, M. A., and Acosta Hospitaleche, C. (2018). Ontogenetic variations of the head of *Aptenodytes forsteri* (Aves, Sphenisciformes): muscular and skull morphology. *Polar Biol.* 41, 225–235. doi:10.1007/s00300-017-2183-3

Starck, J. M., and Ricklefs, R. E. (1998a). *Avian growth and development*. New York, NY: Oxford University Press.

Starck, J. M., and Ricklefs, R. E. (1998b). "Patterns of development: the altricial-precocial spectrum," in *Avian growth and development. Evolution in the altricial precocial spectrum*. Editors J. M. Starck and R. E. Ricklefs (New York, NY: Oxford University Press), 3–30.

Tamura, K., Nomura, N., Seki, R., Yonei-Tamura, S., and Yokoyama, H. (2011). Embryological evidence identifies wing digits in birds as digits 1, 2, and 3. *Science* 331, 753–757. doi:10.1126/science.1198229

Tumarkin-Deratzian, A. R., Vann, D. R., and Dodson, P. (2006). Bone surface texture as an ontogenetic indicator in long bones of the Canada goose *Branta canadensis* (Anseriformes: anatidae). *Zool. J. Linn. Soc.* 148, 133–168. doi:10.1111/j.1096-3642.2006.00232.x

Vargas, A. O., and Fallon, J. F. (2005). Birds have dinosaur wings: the molecular evidence. *J. Exp. Zool.* 304B, 86–90. doi:10.1002/jez.b.21023

Wagner, G. P., and Gauthier, J. A. (1999). 1,2,3 = 2,3,4: a solution to the problem of the homology of the digits in the avian hand. *Proc. Natl. Acad. Sci.* 96, 5111–5116. doi:10.1073/pnas.96.9.5111

Wang, J., Hao, X., Kundrát, M., Liu, Z., Uesugi, K., Jurašeková, Z., et al. (2019b). Bone tissue histology of the Early Cretaceous bird *Yanornis*: evidence for a diphyletic origin of modern avian growth strategies within Ornithuromorpha. *Hist. Biol.* 32, 1422. doi:10.1080/08912963.2019.1593405

Wang, M., Li, Z., and Zhou, Z. (2017b). Insight into the growth pattern and bone fusion of basal birds from an Early Cretaceous enantiornithine bird. *Proc. Natl. Acad. Sci. U.S.A.* 114, 11470–11475. doi:10.1073/pnas.1707237114

Wang, M., O'Connor, J. K., and Zhou, Z. (2019a). A taxonomical revision of the confuciusornithiformes (aves: Pygostylia). *Vertebr. Palasiat.* 57, 1–37. doi:10.19615/j.cnki.1000-3118.180530

Wang, M., Stidham, T. A., and Zhou, Z. (2018a). A new clade of basal Early Cretaceous pygostylian birds and developmental plasticity of the avian shoulder girdle. *Proc. Natl. Acad. Sci. USA* 115, 10708–10713. doi:10.1073/pnas.1812176115

Wang, M., Zheng, X., O'Connor, J. K., Lloyd, G. T., Wang, X., Wang, Y., et al. (2015). The oldest record of Ornithuromorpha from the early cretaceous of China. *Nat. Commun.* 6, 6987. doi:10.1038/ncomms7987

Wang, M., and Zhou, Z. (2017c). A morphological study of the first known piscivorous enantiornithine bird from the Early Cretaceous of China. *J. Vertebr. Paleontol.* 37, e1278702. doi:10.1080/02724634.2017.1278702

Wang, M., and Zhou, Z. (2017b). A new adult specimen of the basalmost ornithuromorph bird *Archaeorhynchus spathula* (Aves: ornithuromorpha) and its implications for early avian ontogeny. *J. Syst. Palaeontology* 15, 1–18. doi:10.1080/14772019.2015.1136968

Wang, M., and Zhou, Z. (2017a). "The evolution of birds with implications from new fossil evidences," in *The biology of the avian respiratory system*. Editor J. N. Maina (Basingstoke, United Kingdom: Springer Nature), 1–26.

Wang, M., and Zhou, Z. (2017b). A new basal ornithuromorph bird (Aves: Ornithothoraces) from the Early Cretaceous of China with implication for morphology of early Ornithuromorpha. *Zool. J. Linn. Soc.* 176, 207–223. doi:10.1111/zoj.12302

Wang, X., Chiappe, L. M., Teng, F., and Ji, Q. (2013a). *Xinghaiornis lini* (Aves: Ornithoraces) from the early cretaceous of liaoning: an example of the evolutionary mosaic in early birds. *Acta Geol. Sin.* 87, 686–689. doi:10.1111/1755-6724.12080

Wang, X., Ji, Q., Teng, F., and Jin, K. (2013b). A new species of *Yanornis* (aves: ornithurae) from the lower cretaceous strata of yixian, liaoning province. *Geol. Bull. China* 32, 601–606.

Wang, X., O'Connor, J. K., Zhao, B., Chiappe, L. M., Gao, C., and Cheng, X. (2010). New species of Enantiornithes (aves: Ornithothoraces) from the qiaotou formation in northern Hebei, China. *Acta Geol. Sin.* 84, 247–256. doi:10.1111/j.1755-6724.2010.00156.x

Wang, X., O'Connor, J. K., Maina, J. N., Pan, Y., Wang, M., Wang, Y., et al. (2018). Archaeorhynchuspreserving significant soft tissue including probable fossilized lungs. *Proc. Natl. Acad. Sci. USA* 115, 11555–11560. doi:10.1073/pnas.1805803115

Wang, Y., Hu, H., O'Connor, J. K., Wang, M., Xu, X., Zhou, Z., et al. (2017). A previously undescribed specimen reveals new information on the dentition of *Sapeornis chaoyangensis*. *Cretaceous Res.* 74, 1–10. doi:10.1016/j.cretres.2016.12.012

Wellnhofer, P. (2009). *Archaeopteryx*: the icon of evolution. München, Germany: Verlag Dr. Friedrich Pfeil.

Wellnhofer, P. (1974). Das fünfte skelettexemplar von *Archaeopteryx*. *Palaeontogr. Abt. A.* 147, 169–216.

Wilson, J. A. (2006). Anatomical nomenclature of fossil vertebrates: standardized terms or "lingua franca"? *J. Vertebr. Paleontol.* 26, 511–518. doi:10.1671/0272-4634(2006)26[511:anofvs]2.0.co;2

Xing, L., O'Connor, J. K., McKellar, R. C., Chiappe, L. M., Bai, M., Tseng, K., et al. (2018). A flattened enantiornithine in mid-Cretaceous Burmese amber: morphology and preservation. *Sci. Bull.* 63, 235–243. doi:10.1016/j.scib.2018.01.019

Xing, L., O'Connor, J. K., McKellar, R. C., Chiappe, L. M., Tseng, K., Li, G., et al. (2017). A mid-Cretaceous enantiornithine (Aves) hatchling preserved in Burmese amber with unusual plumage. *Gondwana Res.* 49, 264–277. doi:10.1016/j.gr.2017.06.001

Young, R. L., Bever, G. S., Wang, Z., and Wagner, G. P. (2011). Identity of the avian wing digits: problems resolved and unsolved. *Dev. Dyn.* 240, 1042–1053. doi:10.1002/dvdy.22595

Zhang, F., Zhou, Z., Hou, L., and Gu, G. (2001). Early diversification of birds: evidence from a new opposite bird. *Chin.Sci.Bull.* 46, 945–949. doi:10.1007/bf02900473

Zhang, L., Yang, Y., Zhang, L., Guo, S., Wang, W., and Zheng, S. (2007). Precious fossil-bearing beds of the lower cretaceous Jiufotang Formation in western liaoning province, China. *Acta Geol. Sin.* 81, 357–364.

Zheng, X., O'Connor, J. K., Wang, X., Wang, Y., and Zhou, Z. (2018). Reinterpretation of a previously described Jehol bird clarifies early trophic evolution in the Ornithuromorpha. *Proc. R. Soc. B.* 285, 20172494. doi:10.1098/rspb.2017.2494

Zheng, X., O'Connor, J. K., Huchzermeyer, F., Wang, X., Wang, Y., Zhang, X., et al. (2014). New specimens of *Yanornis* indicate a piscivorous diet and modern alimentary canal. *PLoS One* 9, e95036. doi:10.1371/journal.pone.0095036

Zheng, X., Wang, X., O'Connor, J. K., and Zhou, Z. (2012). Insight into the early evolution of the avian sternum from juvenile enantiornithines. *Nat. Commun.* 3, 1116. doi:10.1038/ncomms2104

Zhou, S., O'Connor, J. K., and Wang, M. (2014). A new species from an ornithuromorph (Aves: Ornithothoraces) dominated locality of the Jehol Biota. *Chin. Sci. Bull.* 59, 5366–5378. doi:10.1007/s11434-014-0669-8

Zhou, S., Zhou, Z., and O'Connor, J. K. (2012). A new basal beaked ornithurine bird from the Lower Cretaceous of western Liaoning, China. *Vertebr. Palasiat.* 50, 9–24.

Zhou, S., Zhou, Z., and O'Connor, J. K. (2013). Anatomy of the basal ornithuromorph birdArchaeorhynchus spathulafrom the Early Cretaceous of Liaoning, China. *J. Vertebr. Paleontol.* 33, 141–152. doi:10.1080/02724634.2012.714431

Zhou, Z., Clarke, J., Zhang, F., and Wings, O. (2004). Gastroliths in *Yanornis*: an indication of the earliest radical diet-switching and gizzard plasticity in the lineage leading to living birds?. *Naturwissenschaften* 91, 571–574. doi:10.1007/s00114-004-0567-z

Zhou, Z., Li, F. Z. Z., and Li, Z. (2010). A new Lower Cretaceous bird from China and tooth reduction in early avian evolution. *Proc. R. Soc. B* 277, 219–227. doi:10.1098/rspb.2009.0885

Zhou, Z., and Zhang, F. (2006). A beaked basal ornithurine bird (Aves, Ornithurae) from the Lower Cretaceous of China. *Zool Scripta* 35, 363–373. doi:10.1111/j.1463-6409.2006.00234.x

Zhou, Z., and Zhang, F. (2002a). A long-tailed, seed-eating bird from the Early Cretaceous of China. *Nature* 418, 405–409. doi:10.1038/nature00930

Zhou, Z., and Zhang, F. (2005). Discovery of an ornithurine bird and its implication for Early Cretaceous avian radiation. *Proc. Natl. Acad. Sci.* 102. doi:10.1073/pnas.0507106102

Zhou, Z., and Zhang, F. (2002b). Largest bird from the Early Cretaceous and its implications for the earliest avian ecological diversification. *Naturwissenschaften* 89, 34–38. doi:10.1007/s00114-001-0276-9

Conflict of Interest: The authors declare that the research was conducted in the absence of any commercial or financial relationships that could be construed as a potential conflict of interest.